A High Granularity Timing Detector (HGTD) for the ATLAS Experiment at LHC, CERN

By

Usha Mallik (The University of Iowa)

On behalf of the HGTD group

May 24 2018

CALOR 2018, University of Oregon, Eugene, OR

Contents:

Hi-Lumi Phase-II : $7.5x10^{34}$ $cm^{-2}s^{-1}$ (4000 fb^{-1}), pile-up density (μ) 200 in bc of 25 ns
Average interaction density 1.8 vtx/mm (34-200 in 50mm in 150 ps)

Upgrades in Inner Part of ATLAS: ITk (Inner Tracker: Pixel, Si-Strips) and HGTD

ITk covers up to $|\eta| < 4$ with tracking

High pile-up is the biggest challenge in making effective use of the increased luminosity and Phase-II: (better coverage of forward region)

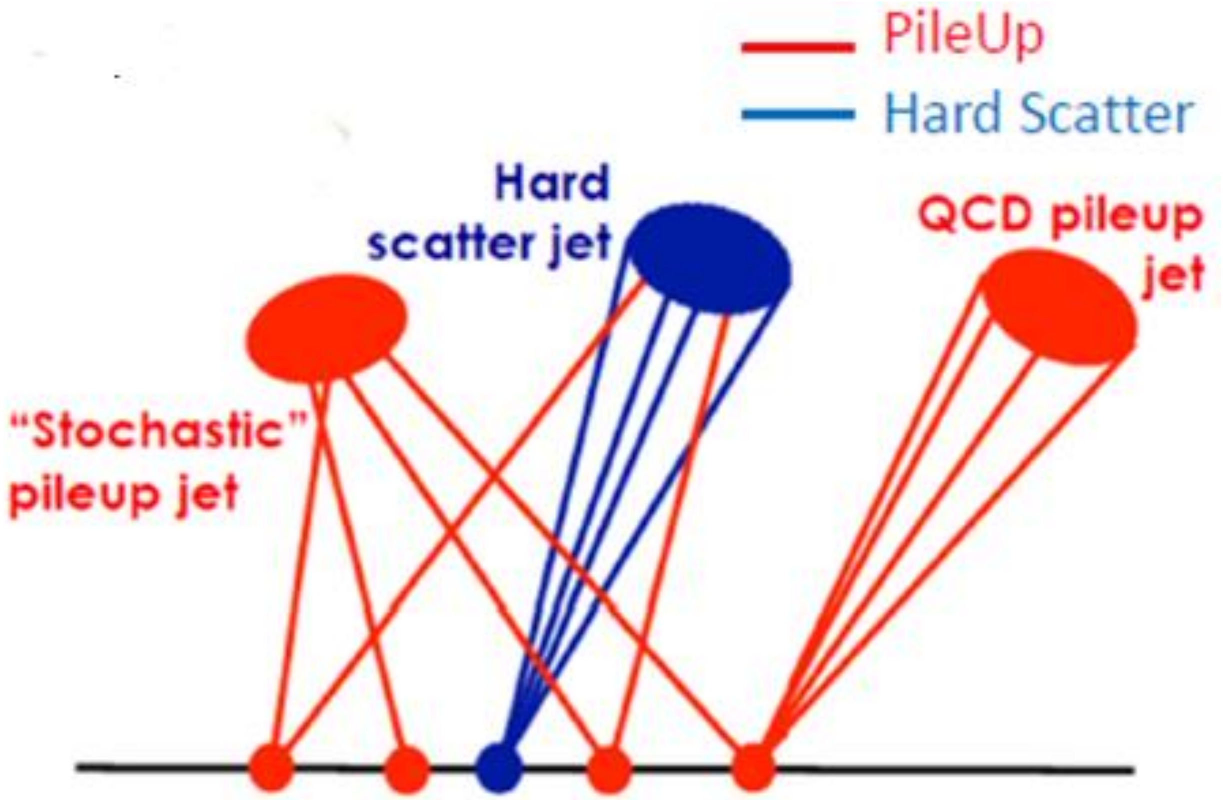

Why Large Rapidity for the HGTD?

At μ = 200 vertex resolution degrades dramatically in the end-cap region, with multiple vertices being merged.

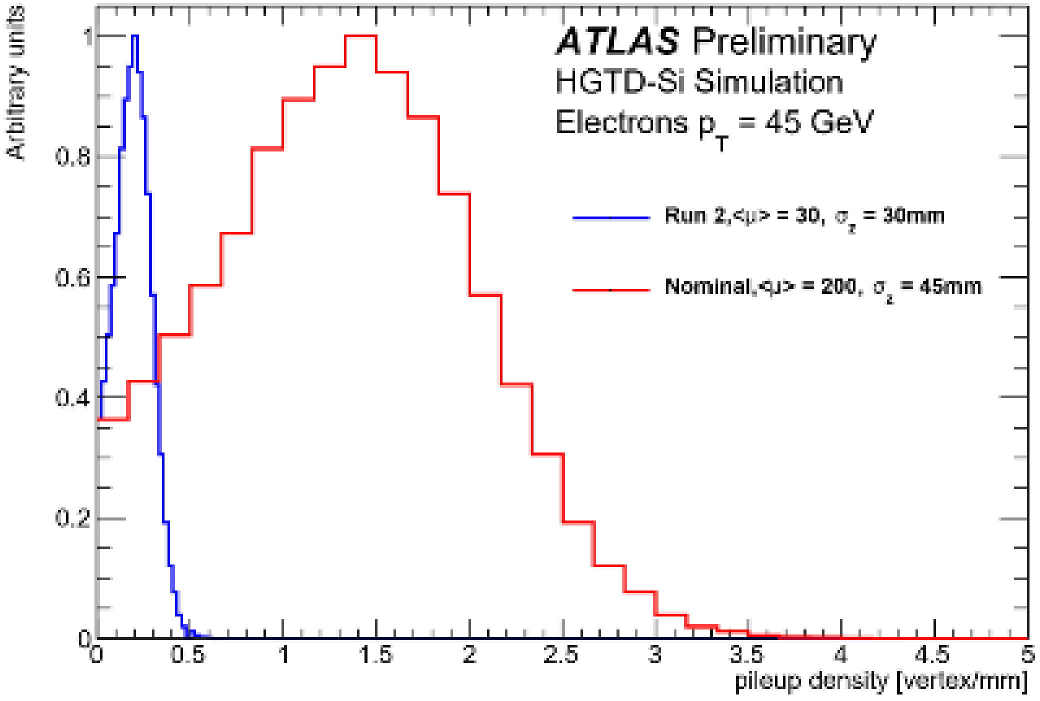

Nominal HL-LHC scenario for <μ> = 30 and <μ> = 200

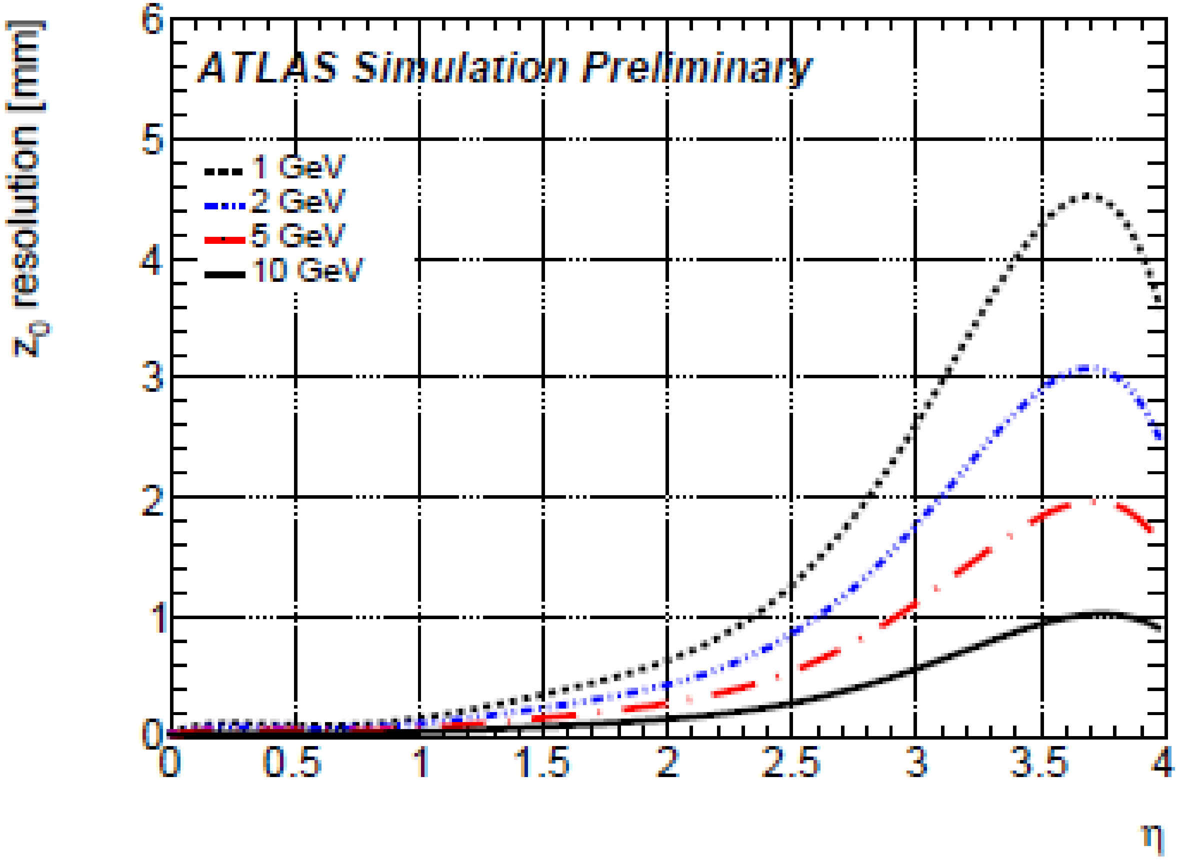

Z0 resolution of the reconstructed vertices

Z-decay width ~ beam spread with HGTD

Final calibration using off-line information; times lined-up across individual pixel-pads of the HGTD using the measured time distribution for many hits. So calibration is determined directly by the beam collision time spectrum and the time of flight to the detector. Width of the distribution provides the motivation for the 30 psec resolution goal (per track)

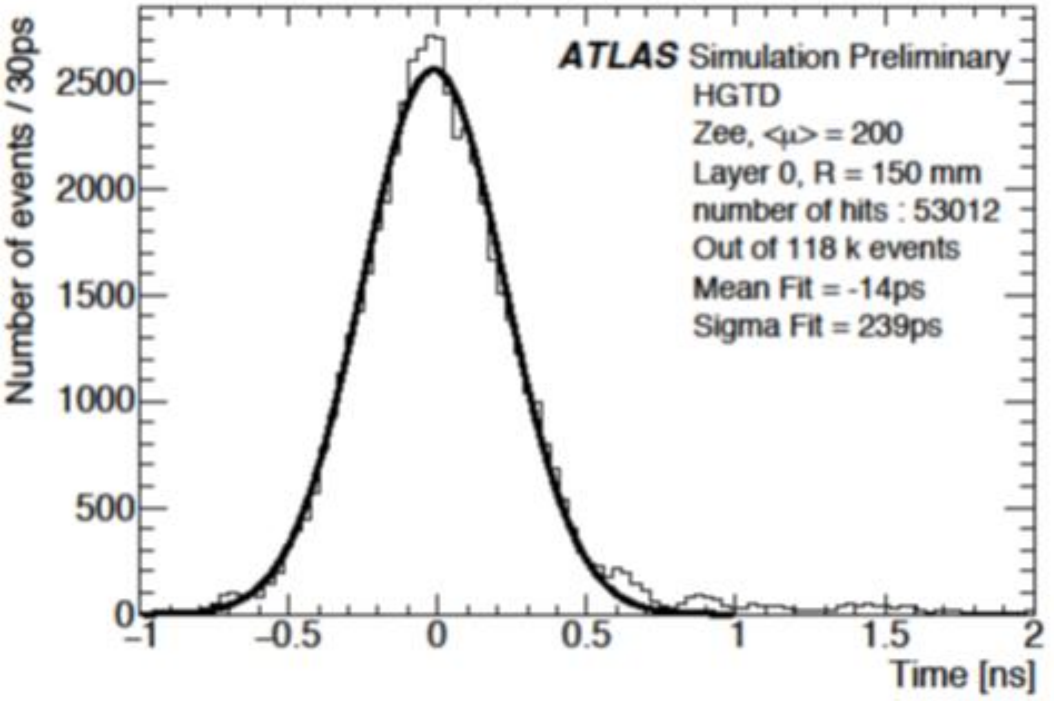

Track to vertex with HGTD, with timing added

Timing provides extra information to collect tracks belonging to the same vertex (with common time of arrival), without actually having to find an accurate vertex in z.

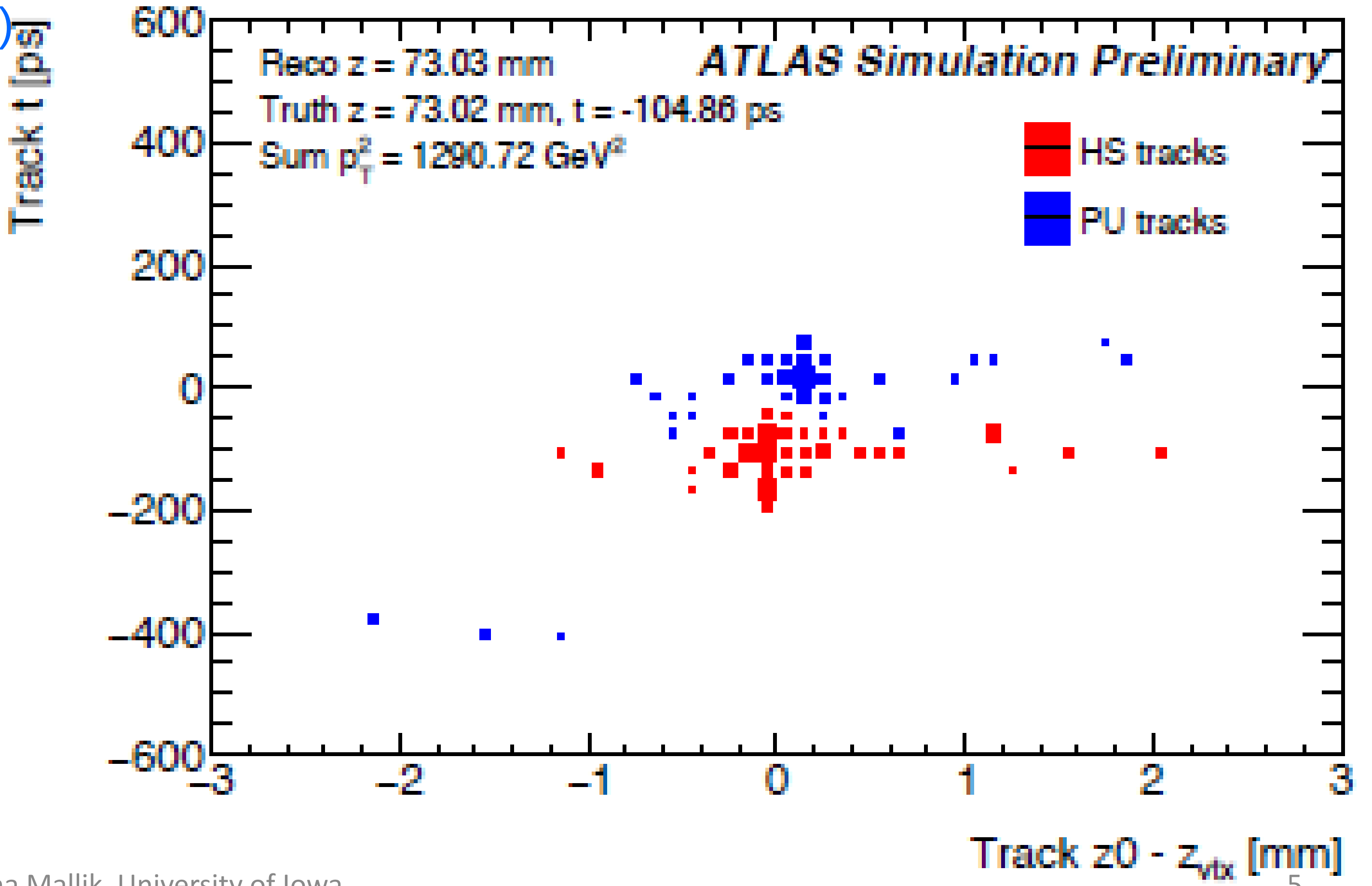

Resolve tracks belonging to close-by vertices

Measure instantaneous luminosity

Provide minimum bias trigger

HGTD: placed between tracker and end-cap calorimeter. Provides time for hits linked with ITk pixel tracks and calorimeter clusters. Common times for tracks nearby in space indicate that they are likely from the same vertex.

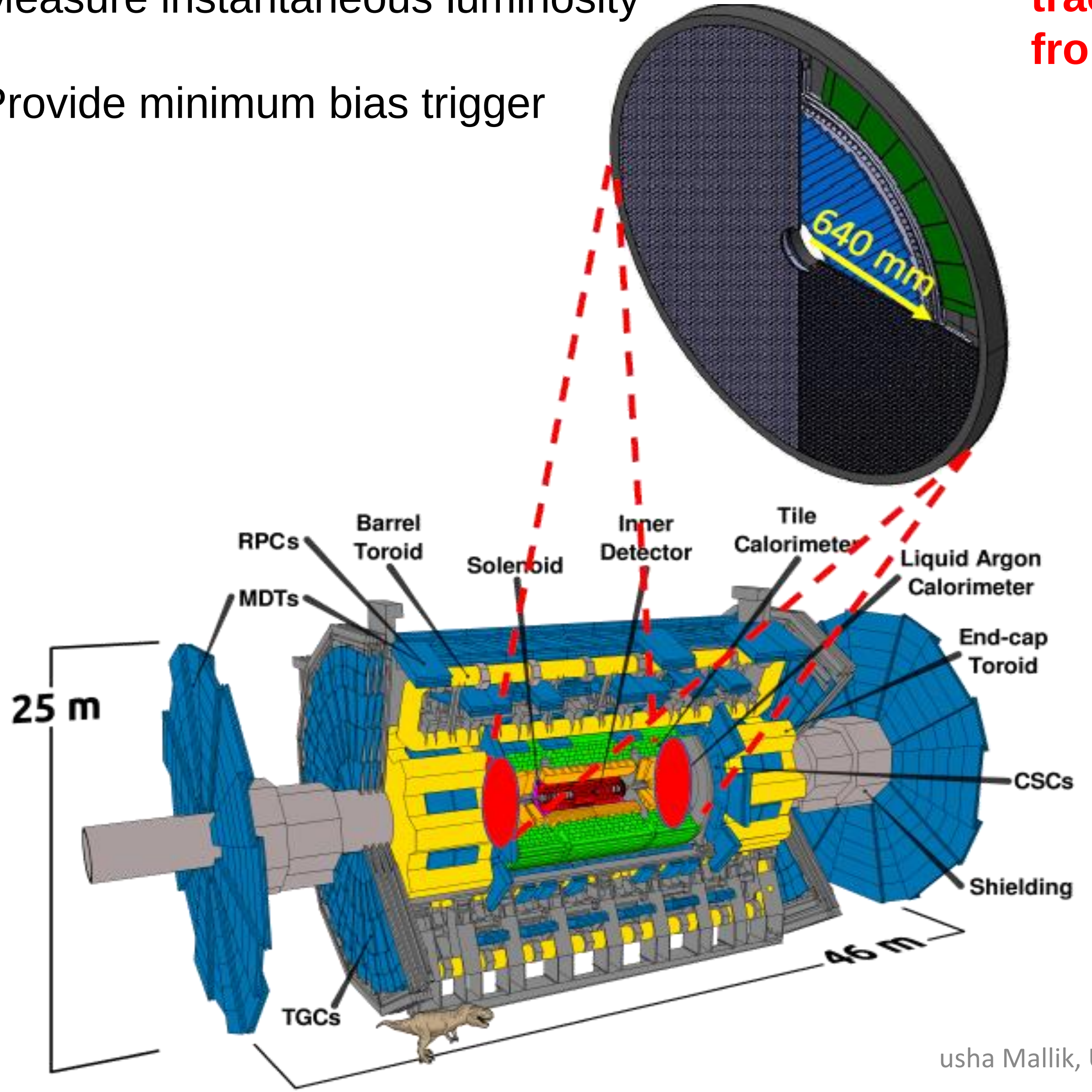

Pseudorapidity coverage	$2.4 < \|\eta\| < 4.0$
Thickness in z	75 mm (+50 mm moderator)
Position of active layers in z	3435 mm $< z <$ 3485 mm
Radial extension:	
Total	110 mm $< R <$ 1000 mm
Active area	120 mm $< R <$ 640 mm
Time resolution per track	30 ps
Number of hits per track:	
$2.4 < \|\eta\| < 3.1$	2
$3.1 < \|\eta\| < 4.0$	3
Pixel size	1.3×1.3 mm^2
Number of channels	3.54M
Active area	6.3 m^2

LGAD (Low Gain Avalanche Detectors) Detectors with Gain and Large Electron Drift Velocity

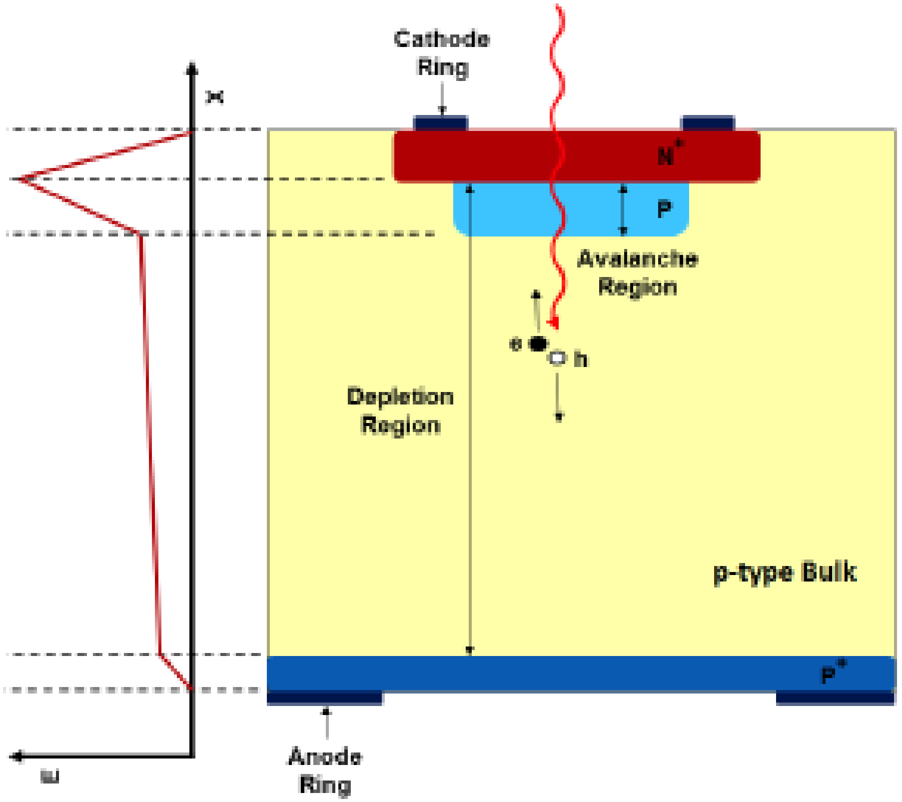

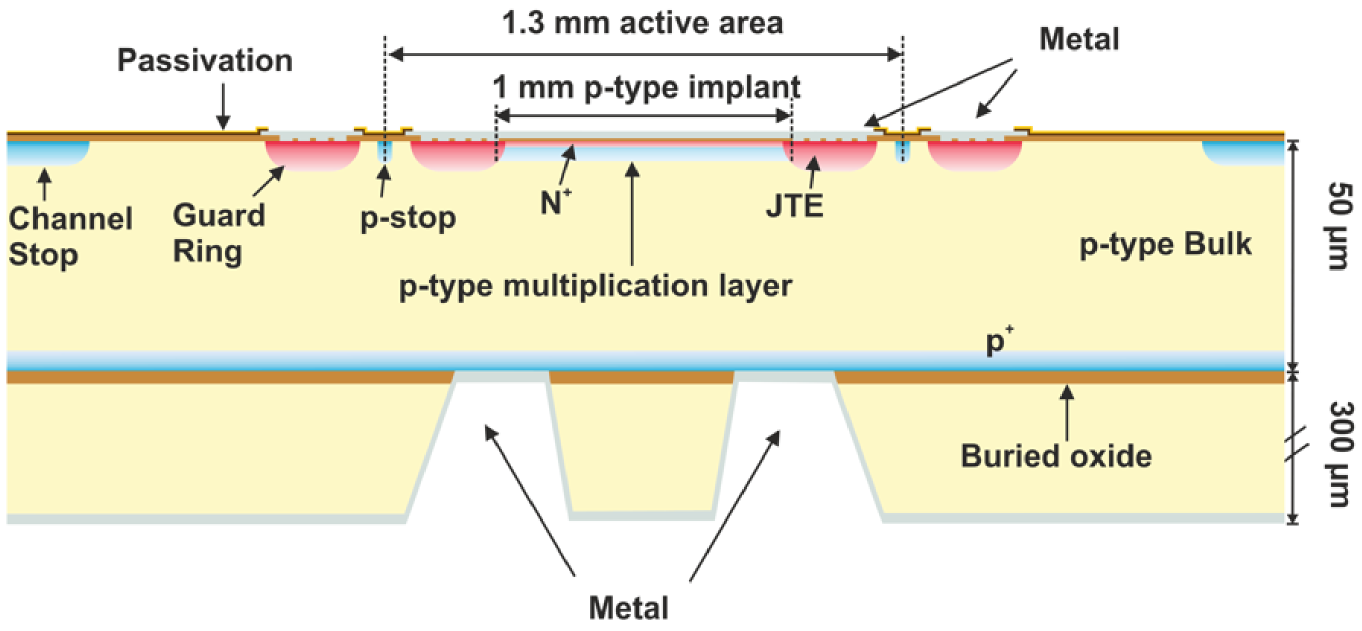

Goal: Gain field ~ 300 kV/cm over a few mm near junction.
Bulk field ~ 20 kV/cm, gives a saturated electron drift velocity ~ 10^7cm/sec. Gain for electrons but not holes, leads to gain ~ 20.

Successful fabrication from CNM, Hamamatsu (HPK), FBK; tested. Also Micron and BNL now.

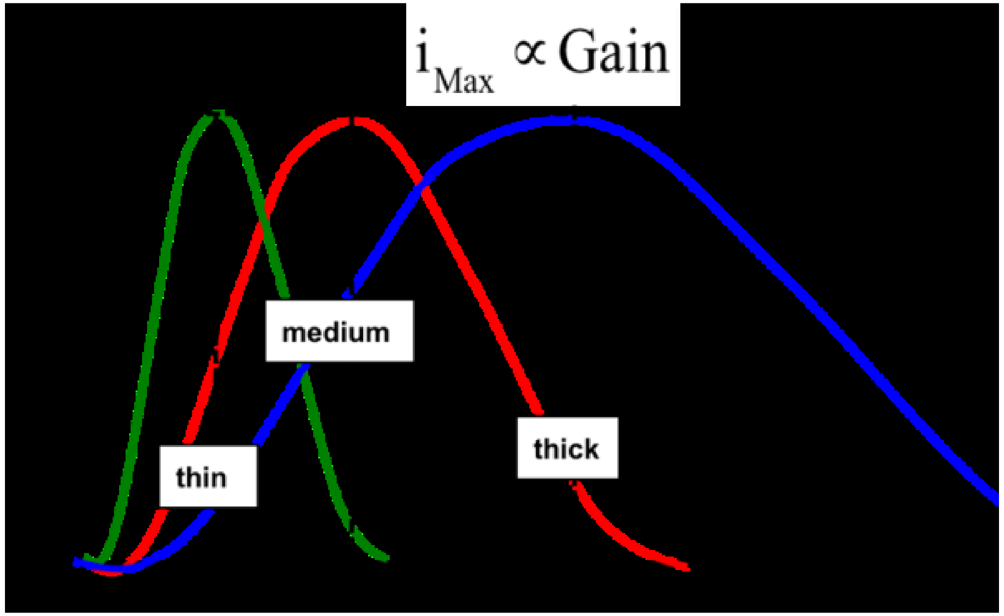

Peak height is independent of thickness, depends on gain

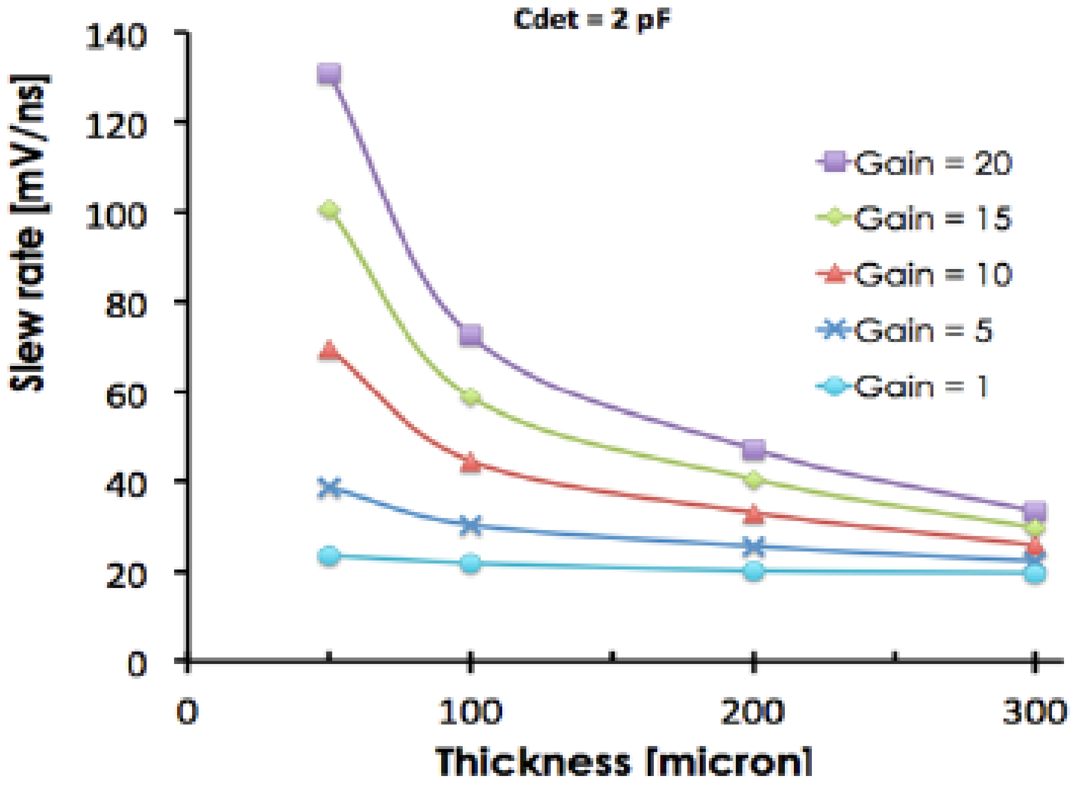

Signal slope vs thickness

Both 50 μm and 35 μm sensor thickness (250 μm support wafer) continue to be tested

Hamamatsu early tests show *the 35 μm sensor would run at 200 volts less than the 50 μm sensor* while maintaining the resolution.

Timing Resolution:

$$\sigma_T^2 = \sigma_L^2 + \sigma_{jitter}^2 + \sigma_{TW}^2 + \sigma_{clock}^2$$

σ_L : Landau fluctuation, depends on deposited charge in sensor, dominates at high gain

σ_{jitter} : Variation from the noise in the signal;

$$\sigma_{jitter}^2 = \frac{N}{dV/dt} \sim \frac{t_{rise}}{S/N}$$

σ_{TW} : Arise from signal of different amplitudes, crossing the threshold at different times
Mitigated by applying corrections from TOT measurement

$$\sigma_{TW}^2 = [\frac{V_{th}}{S/t_{rise}}]_{RMS} \propto [\frac{N}{dV/dt}]_{RMS}$$

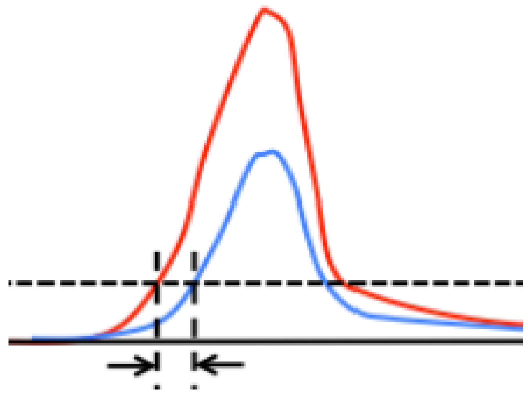

σ_{clock} : Clock distribution, expected to be $\leq$ 10 psec

Some other contributions from TDC and t0 are considered to be negligible.

Some Test beam results: from 2016 ongoing with HPK and CNM sensors (several bench tests performed in addition)

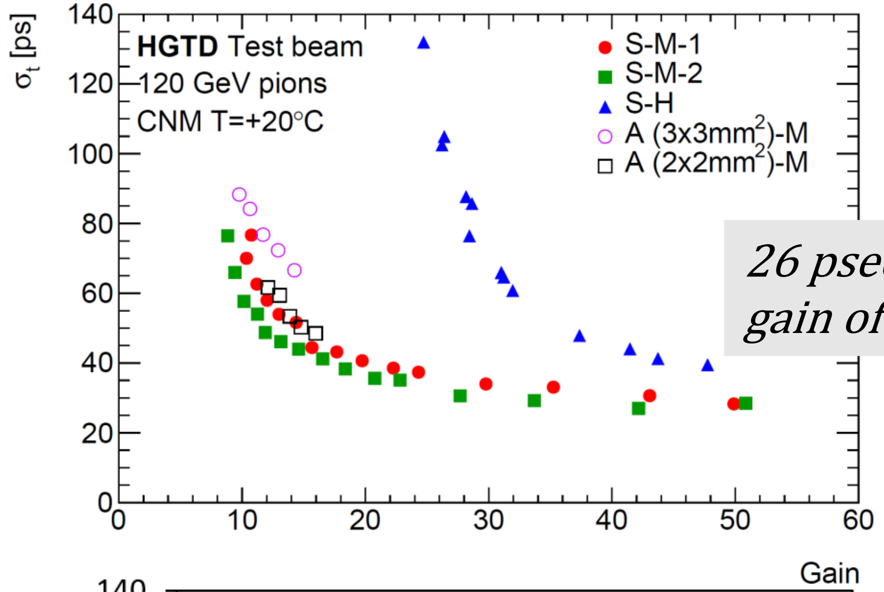

26 psec @ gain of 50

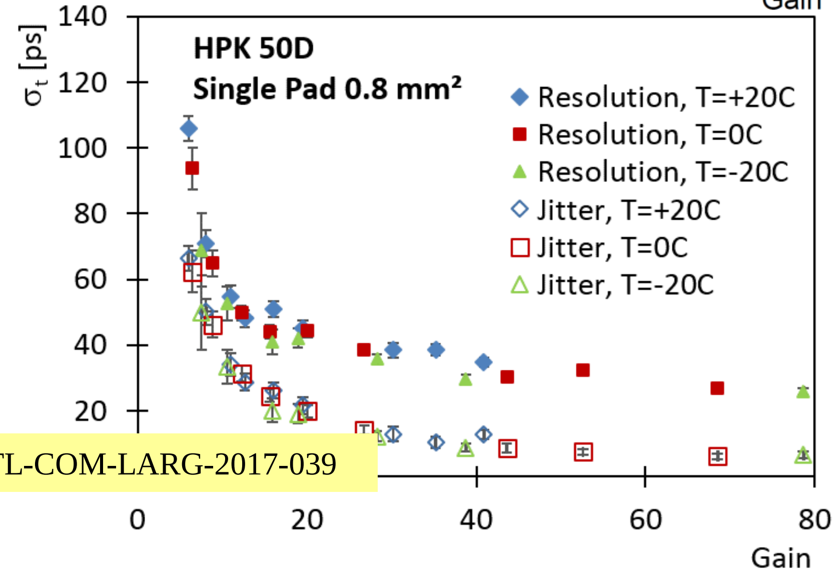

ATL-COM-LARG-2017-039

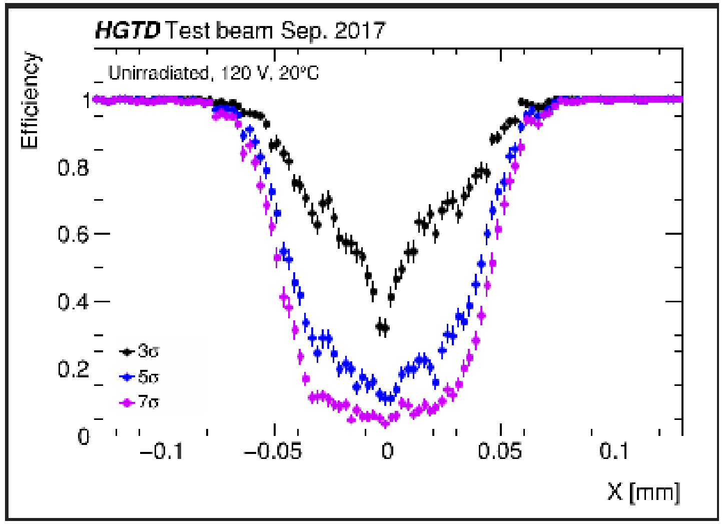

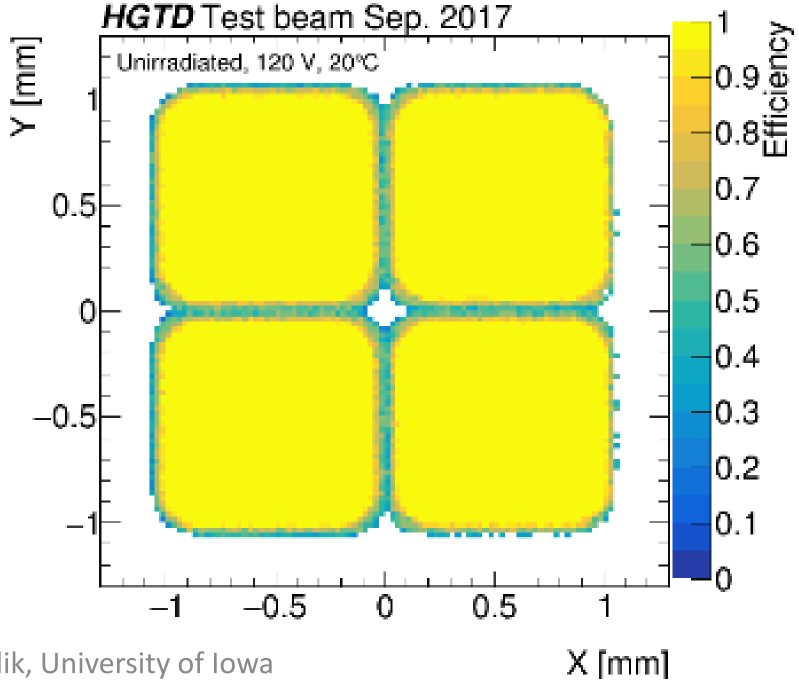

1% efficiency variation

Radiation Hardness :

J. Lange, et al., JINST 12 (2017) P05003

σ_t vs gain

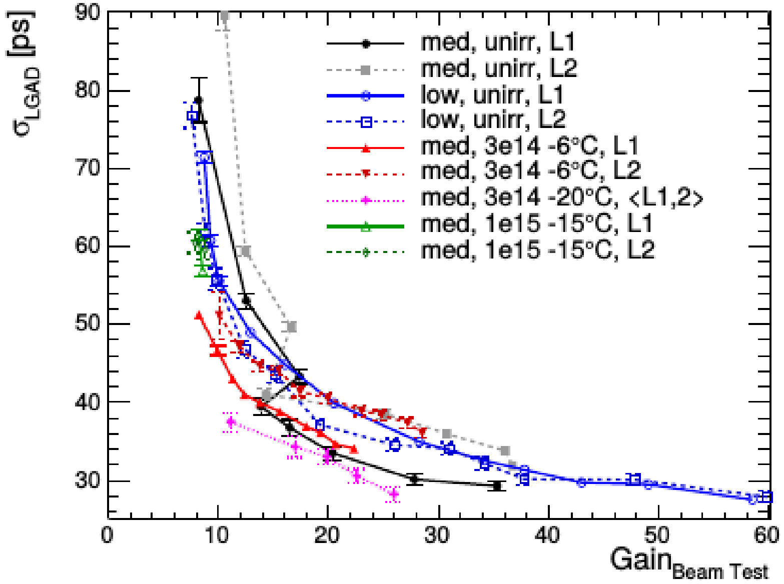

σ_t vs bias voltage

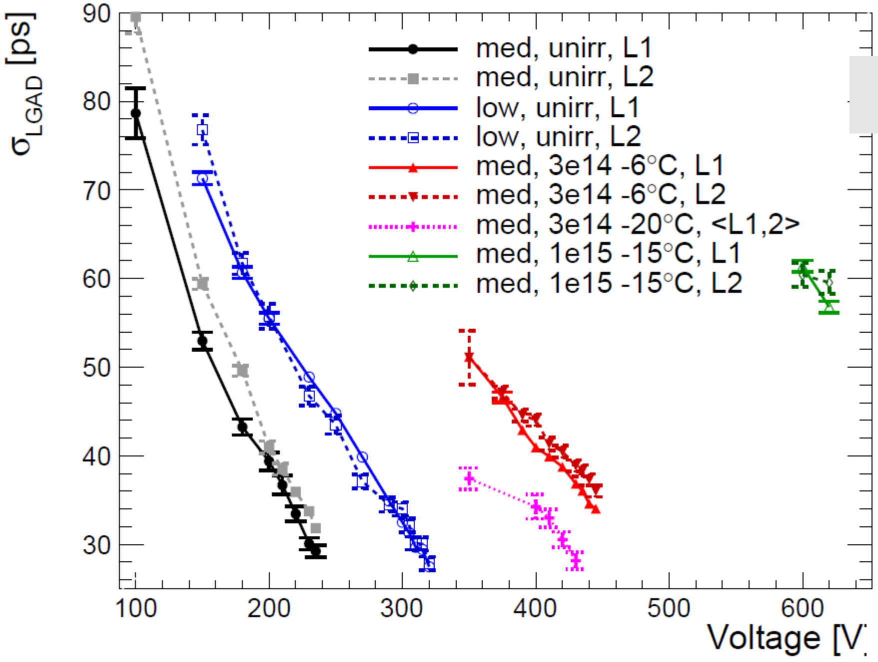

Gain vs bias voltage

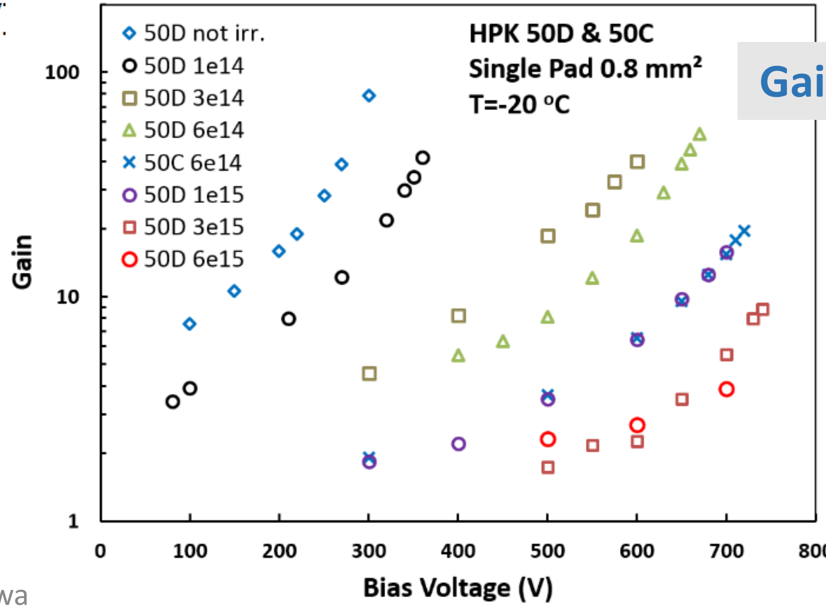

September 2017 test beam with 120 GeV pions at CERN with CNM 2 × 2 arrays, each pad 1.063 × 1.063 mm^2, without and with irradiation https://arxiv.org/abs/1804.00622
Many results with different irradiations and different temperatures ongoing.

Non-irradiated

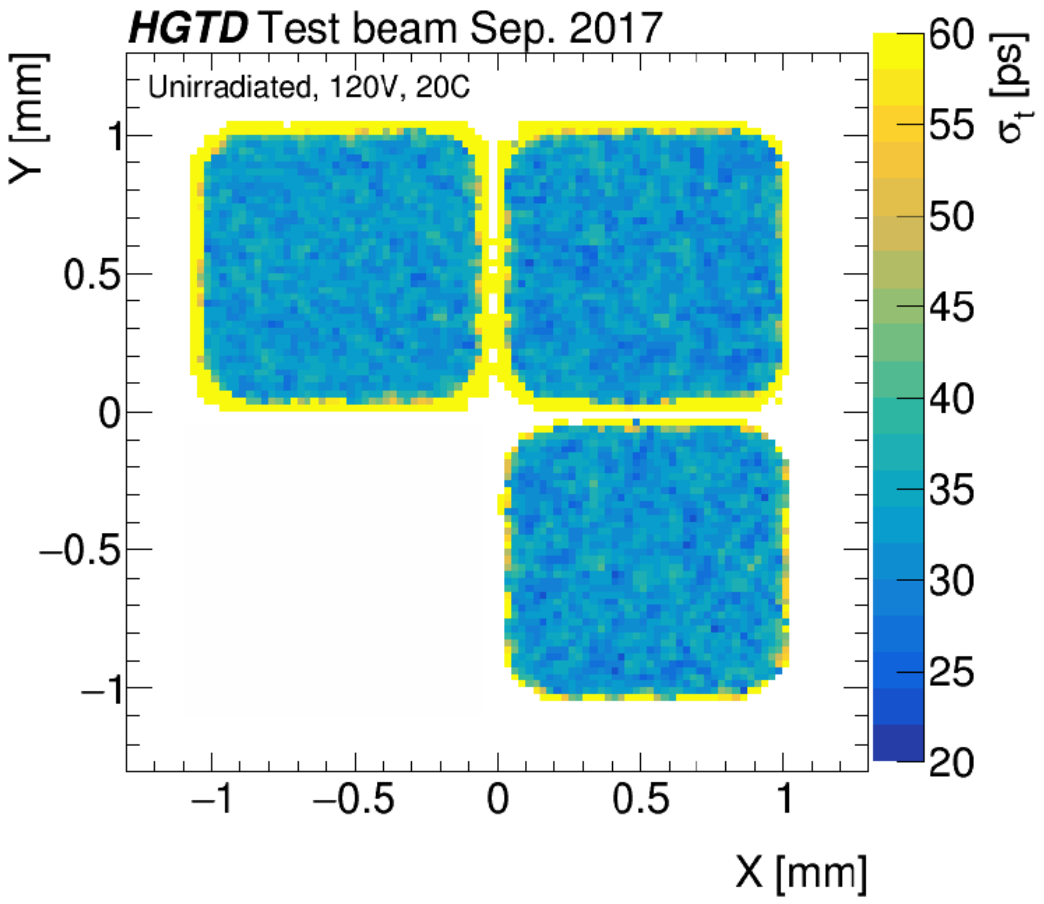

Irradiated

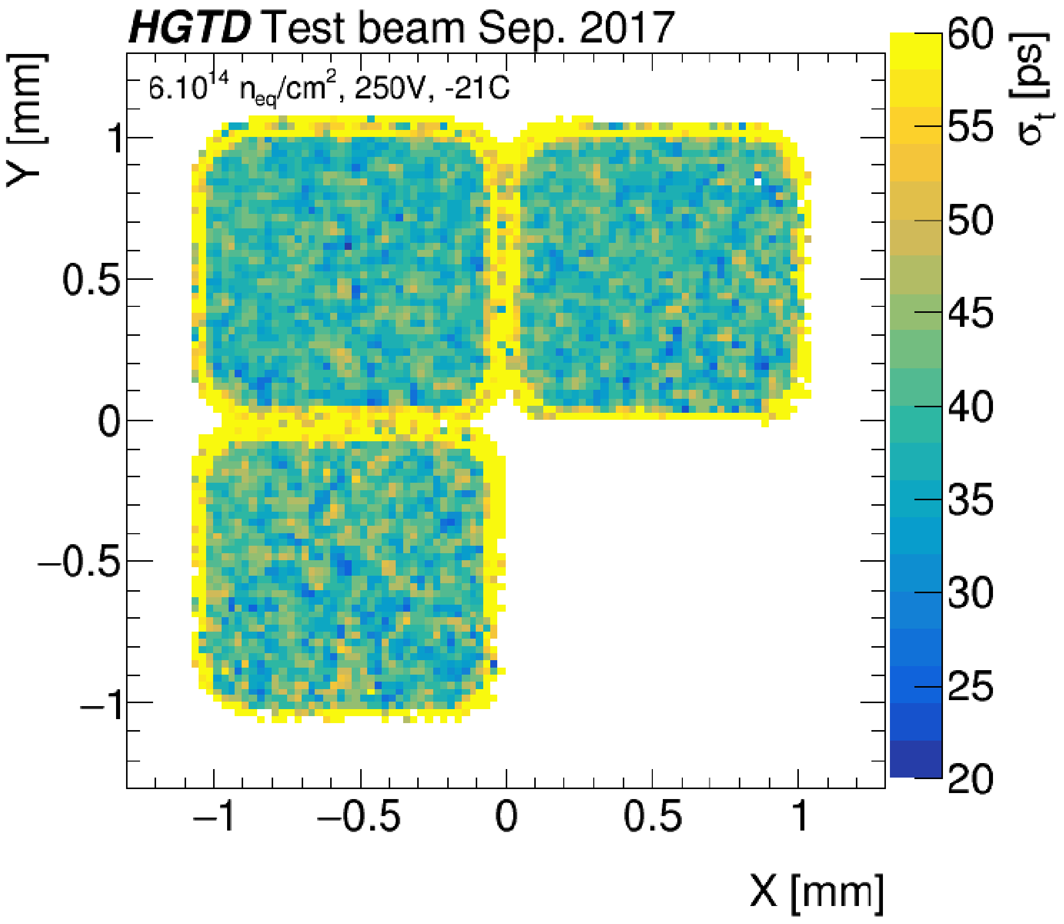

Assembly with (ATLAS LGAD Timing Integrated ReadOut Chip) ALTIROC ASIC Chip:

1.3 × 1.3 mm^2 pixels in 2 × 2 cm^2 die (225 pixels) ASIC, TSMC 130 μm ;
Two ASICs bump-bonded to one 2 × 4 cm^2 sensor
Keep electronic contribution to resolution below 25 psec
Wire bonded to (Kapton) Flex cables

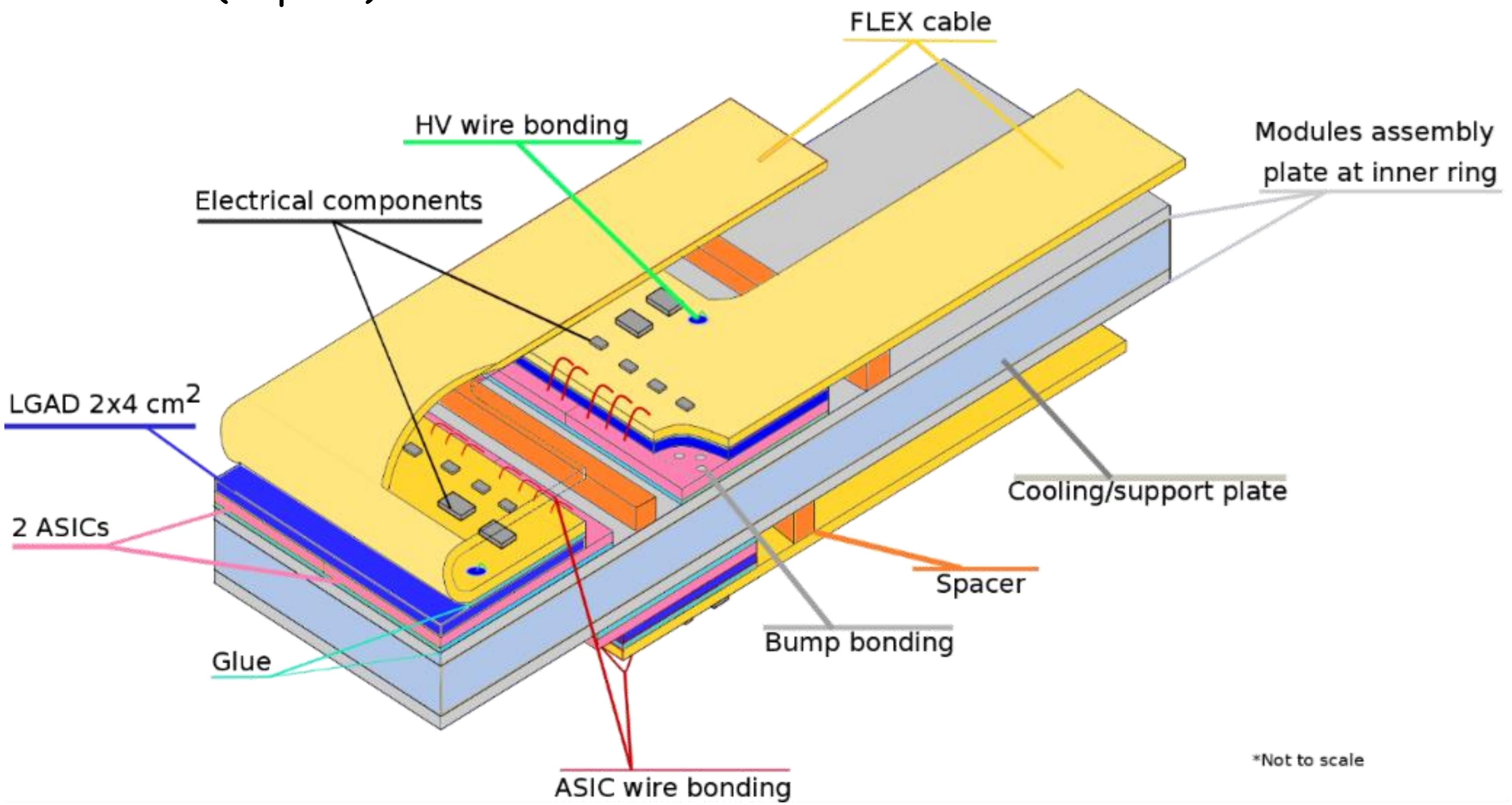

Current Status of ALTIROC:

ALTIROC0 v1: analog single pixel
Test bench studies of ALTIROC0 v2 started with initial promising results
Layout of single channel readout (analog+digital) is finished, post-layout simulations are ongoing
Off-pixel design is ongoing (mainly phase-shifter and luminosity data formatting unit)
5 × 5 version (ALTIROC1) to be submitted in June
(Initial version had CFD, TOT both; CFD is dropped)
Power limit goal: 300 mW/cm^2 ; a fixed threshold discriminator to measure TOA

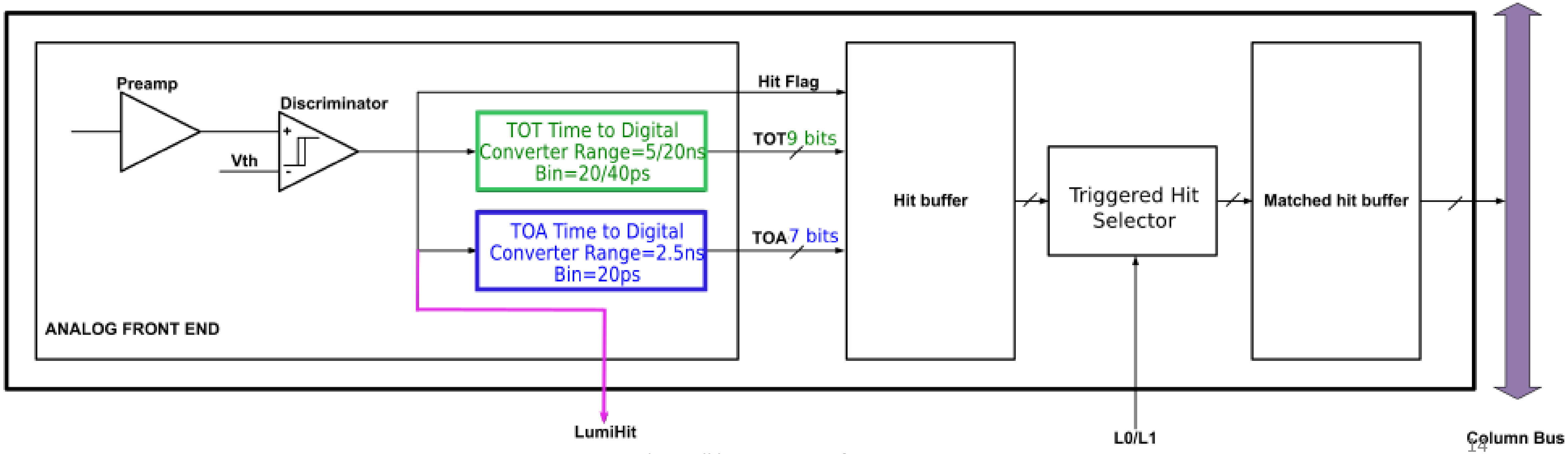

Single Channel Preamp and Discriminator

Rise time optimized to match drift time of sensor (0.5 – 1 nsec), minimizes jitter
Voltage/VPA and transimpedance/TZ have been implemented in simulation
TOT excursion of the TZ is much shorter, and jitter is higher
Simulated/measured jitter in VPA below 15/25 ps for 1 MIP

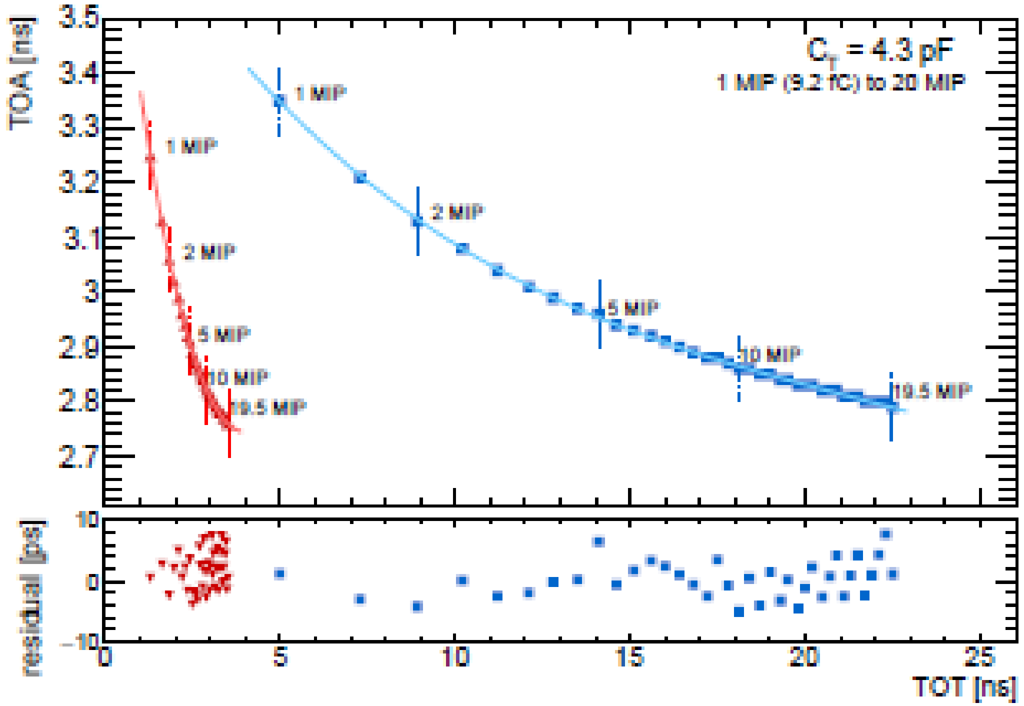

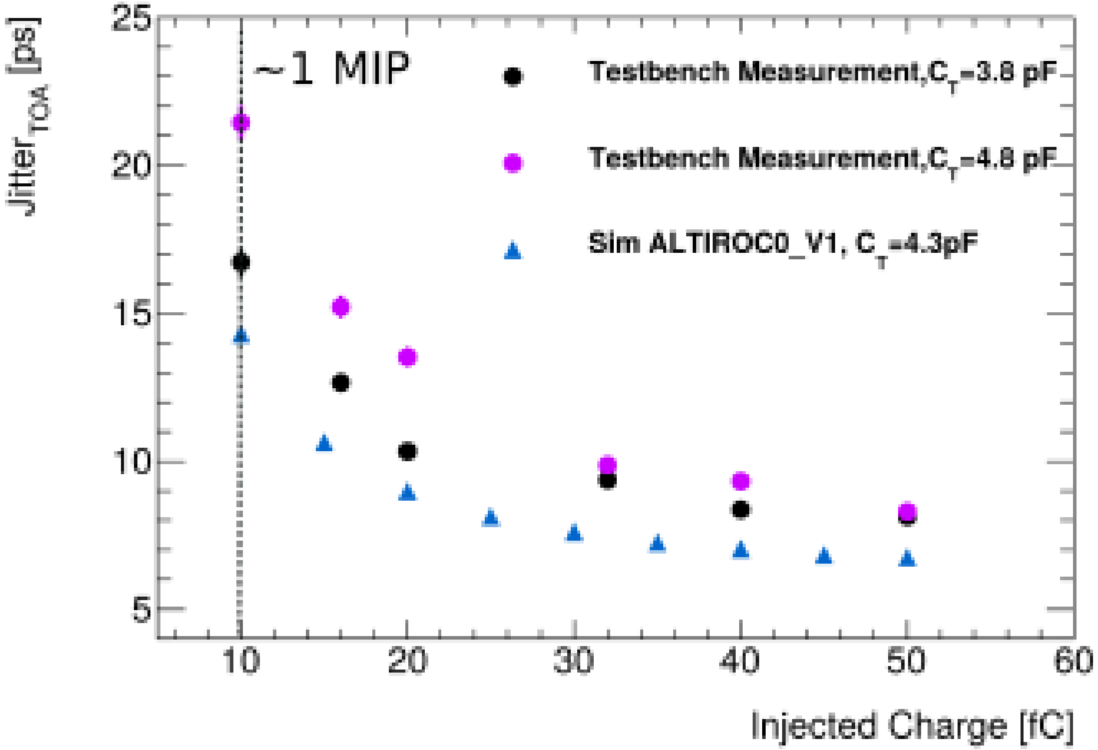

Time walk correction is minimal (<10 ps, peak to peak) for all values of MIP (1 -20 MIPs)

ReadOut Chain from HGTD

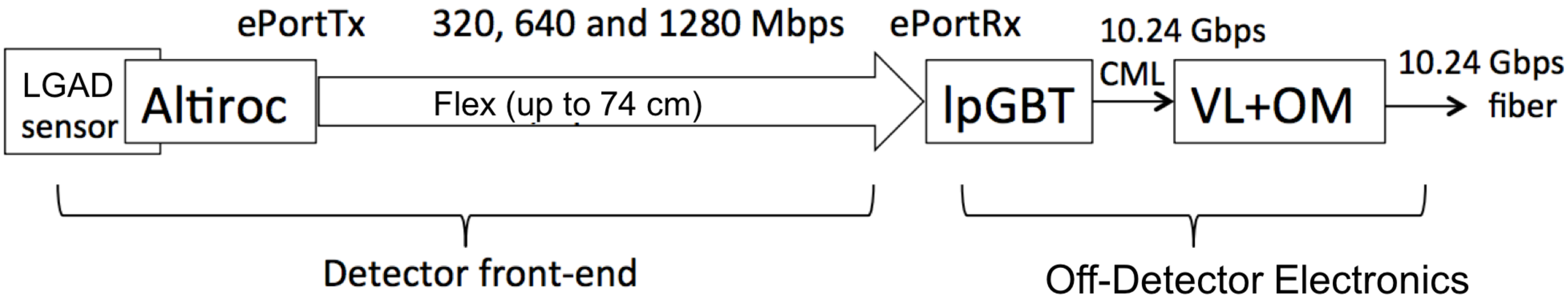

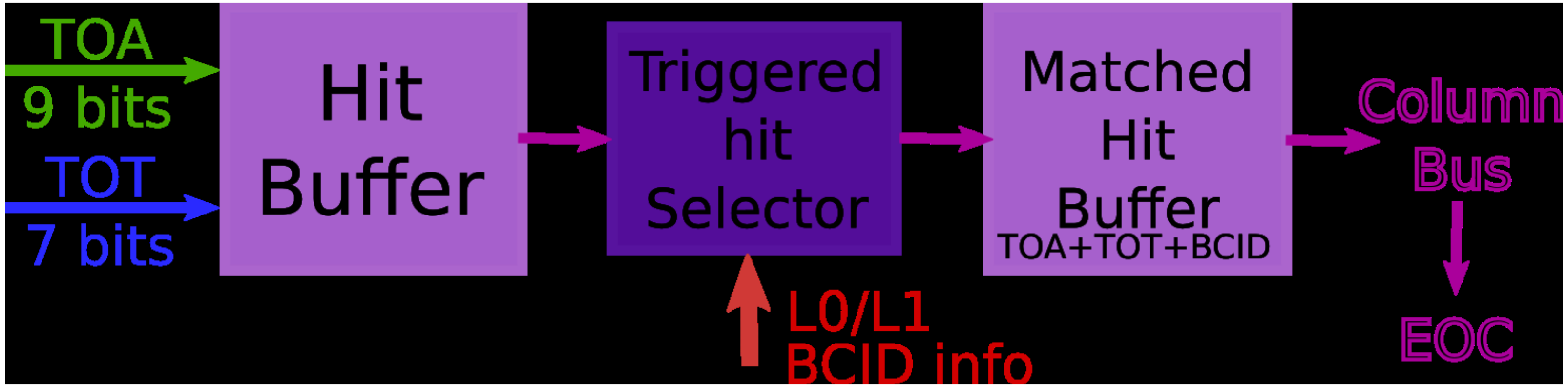

StoreTOA+TOT/hit flag:

Handle 10/35 μs latency for L0/L1 trigger

Forward & backward detector disks with central half rings & stave concept.
Total 6 m^2 LGAD sensors ~ 7888 modules in total
2 x 4 cm^2 per module

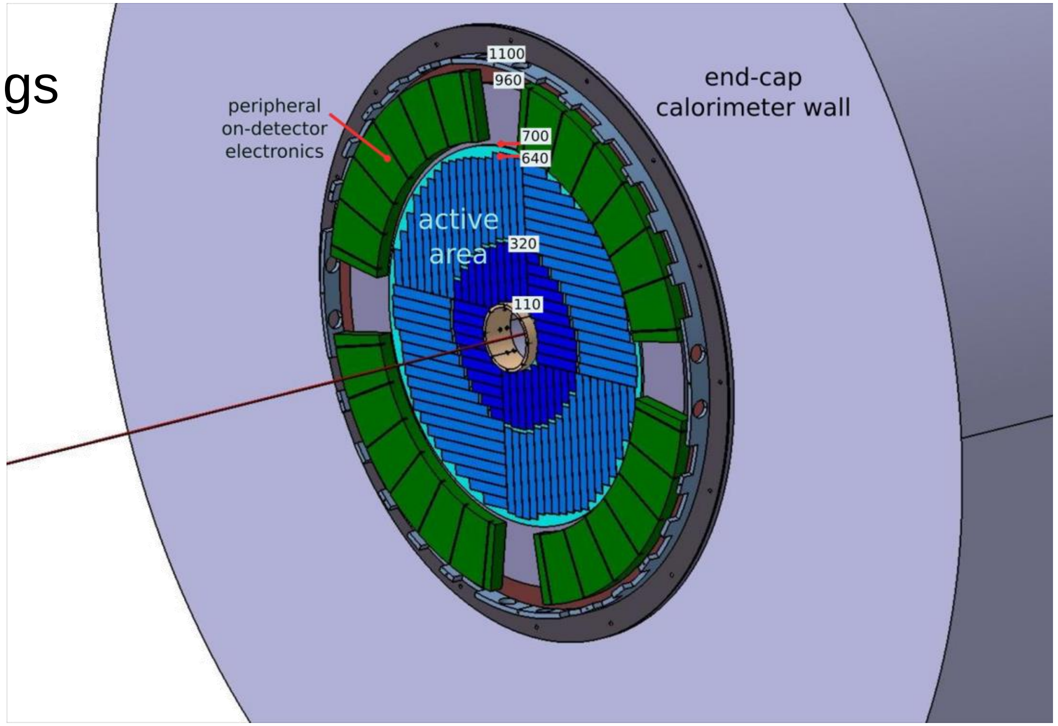

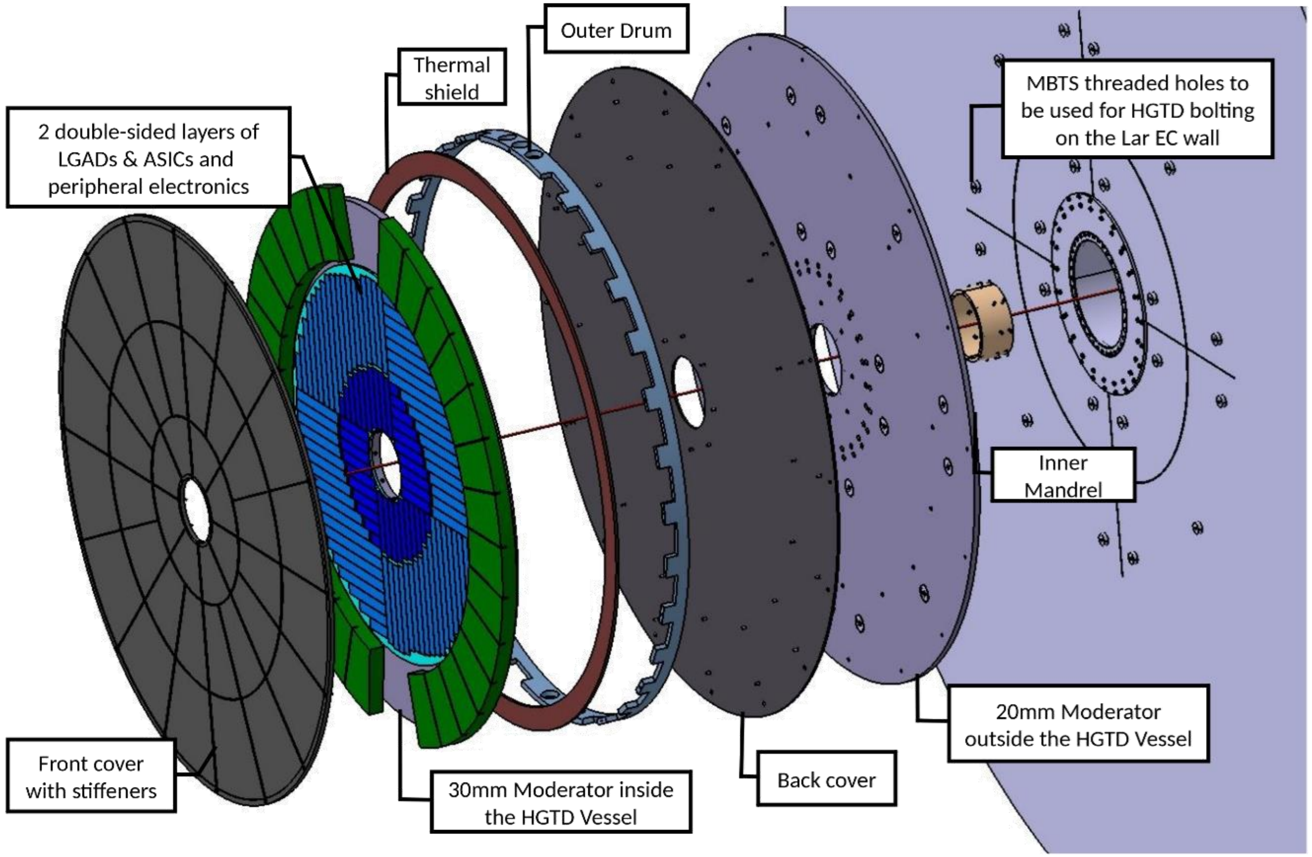

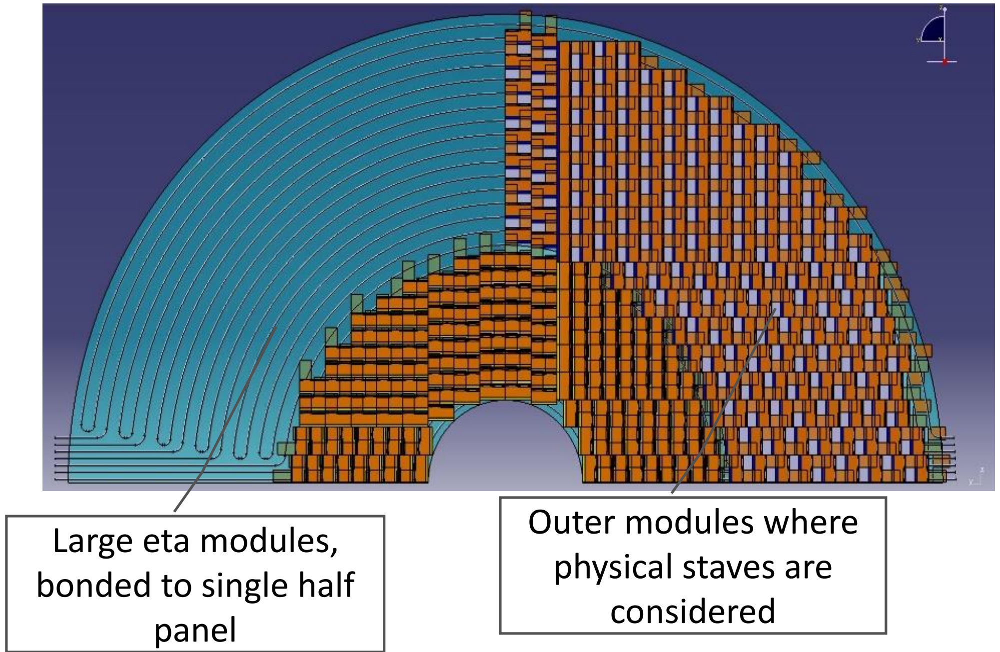

Layout Optimization

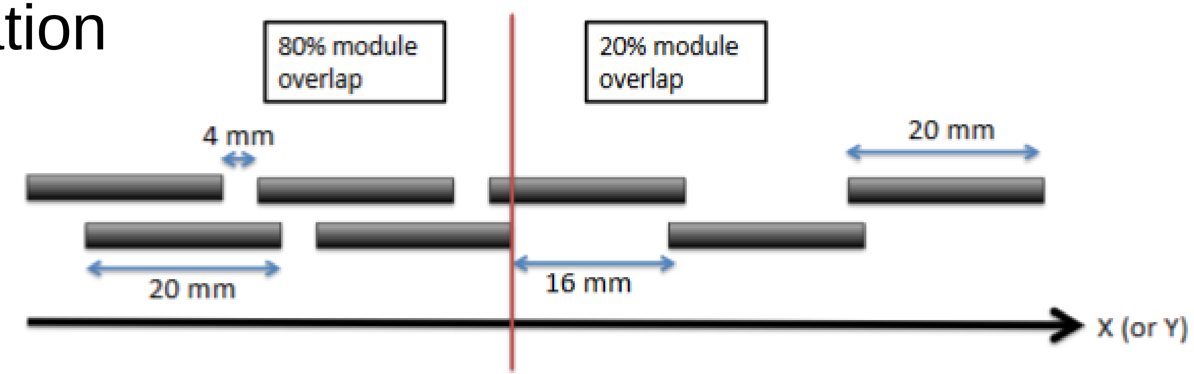

Modules are partially overlapped.To deal with worsening time resolution after large irradiation to the small radius sensors overlap is much larger (80%) in the inner region. Leads typically to an additional hit in this region.

Stave layout

Efficiency		Geometry	
Events with 0 hits	0.7 %	Longest Stave	546 mm
Fraction of events at x or y = 0	52 %	Coverage	91.8 %
		18 staves per quadrant	

Sensor Overlap

- Resolution degrades with irradiation
- Inner region more affected

Fill Factor

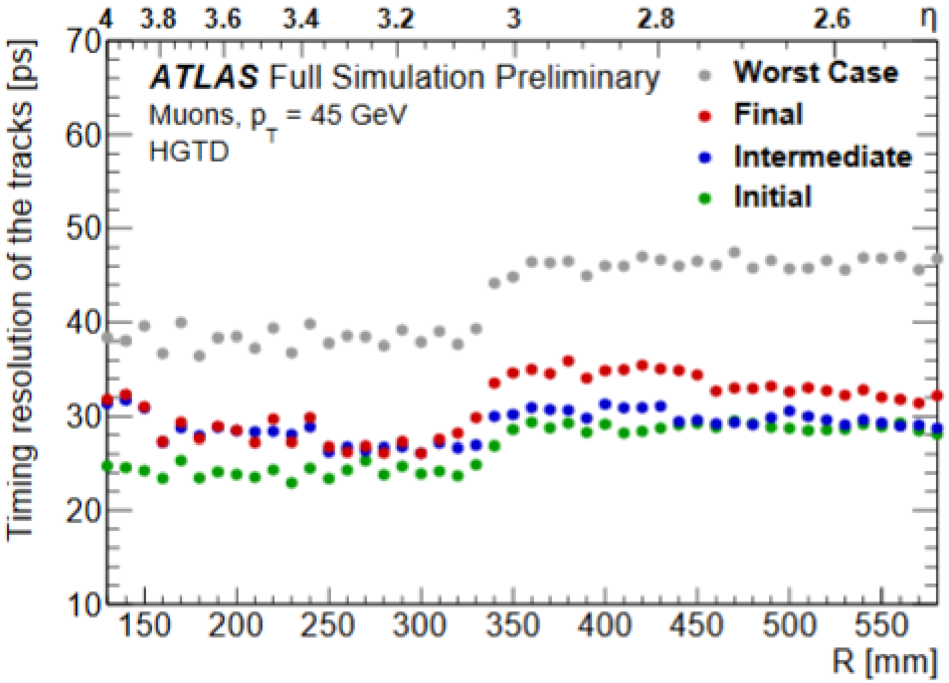

Inter-pad Region

30 µm → 94 %
50 µm → 90 %
100 µm → 82 %

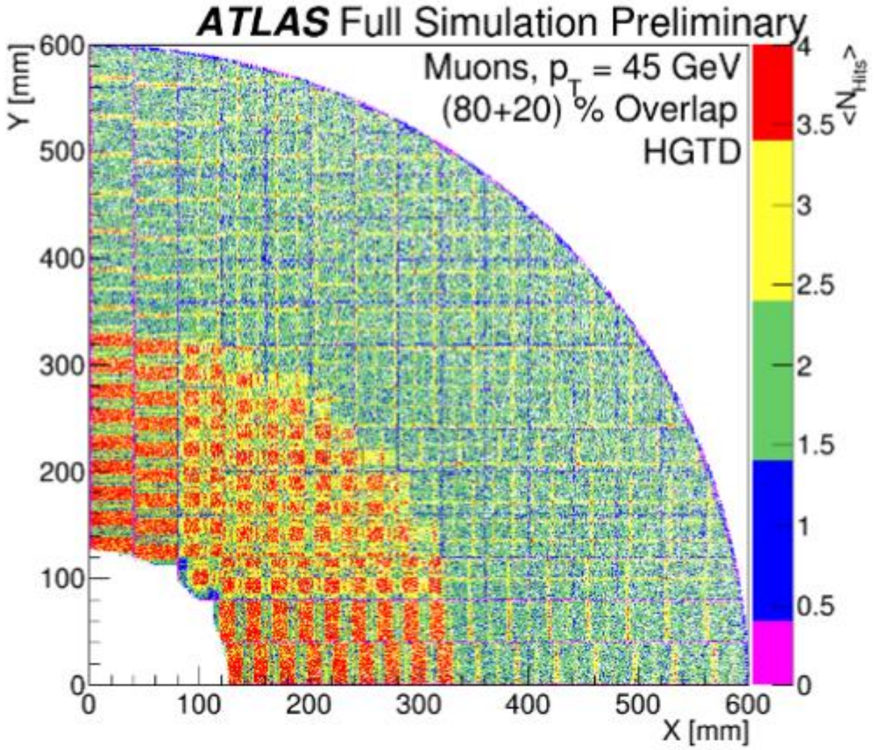

Physics-related Performance Improvement with HGTD

Jet finding Efficiency

Important for finding jets in high |η| region

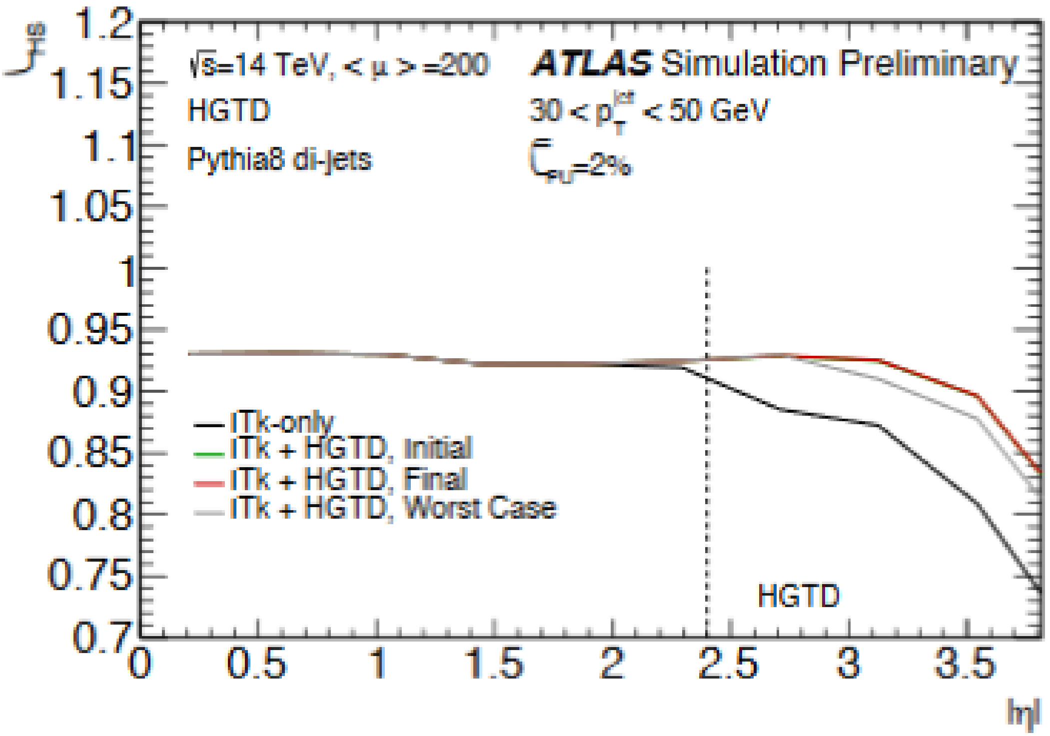

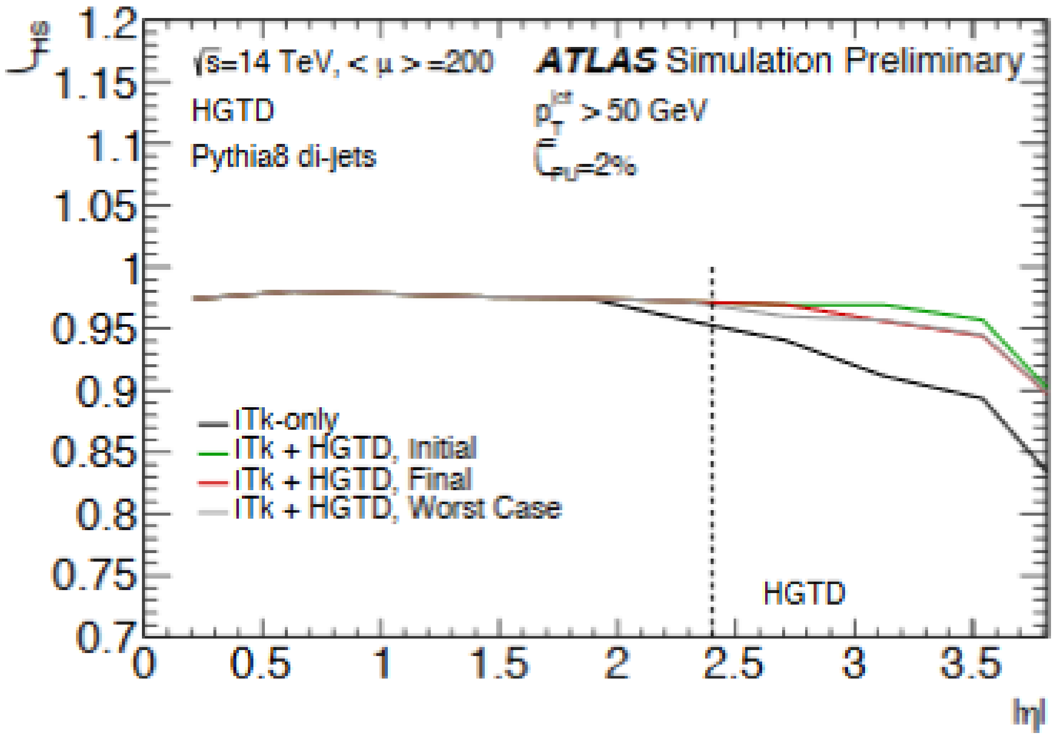

Hard scatter jet efficiency for 2% pileup-jet efficiency. With HGTD, performance nearly independent of rapidity; shown for different time periods with anticipated modest changes in resolution due to radiation damage.

Improvement in b-tagging Efficiency

Important for tagging b-jets in high |η| region; HGTD provides a much better light-jet rejection than the ITk alone for large rapidities (factor of 3 for 70% efficiency working point).

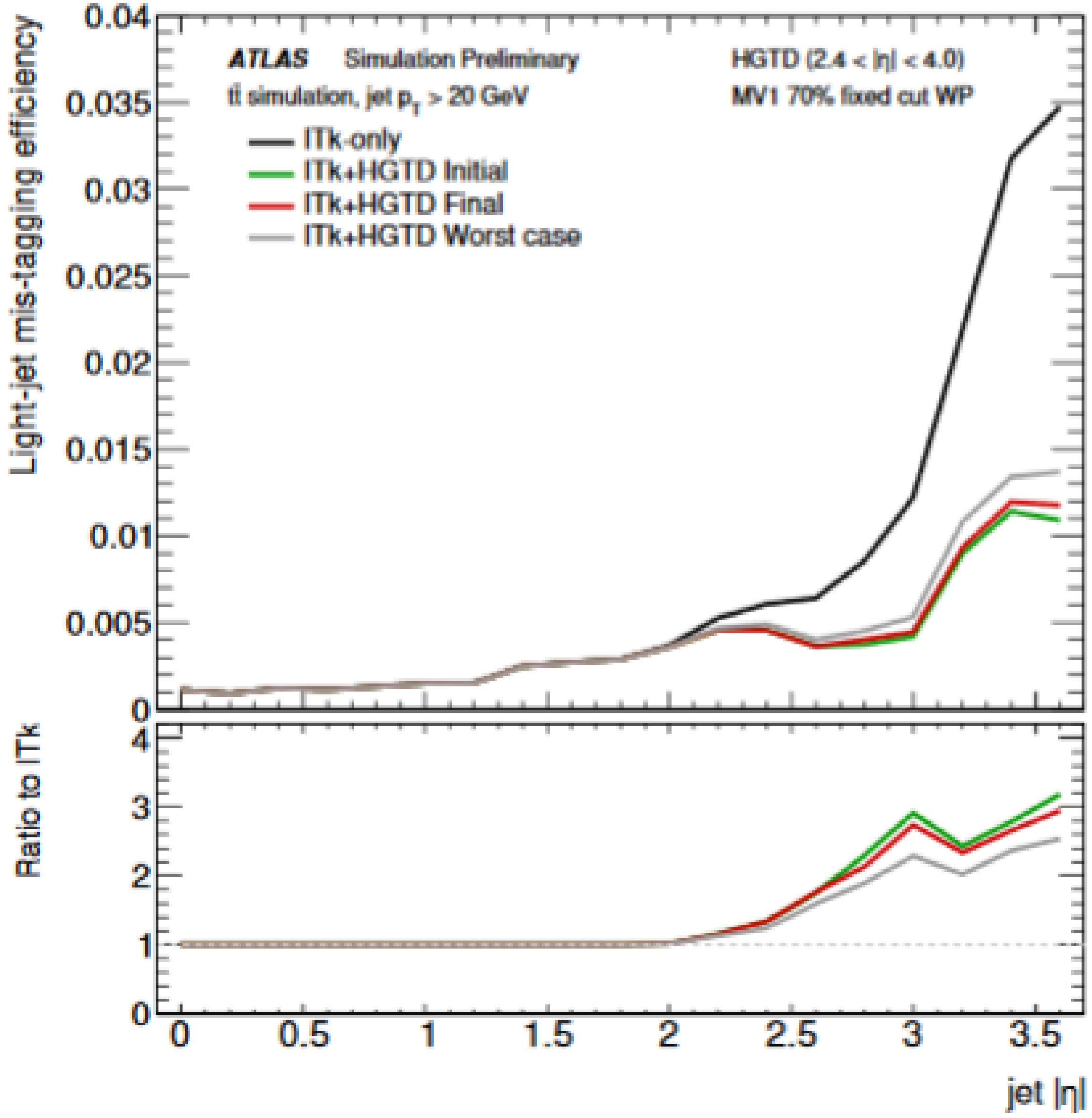

Light-jet mis-tag rate for a 70% b-tagging efficiency working point.

Electron Isolation Efficiency vs pileup density (vertices/mm)

for different timing resolutions

The various performance improvements for physics objects yield typically a 10% improvement in sensitivity across a broad number of physics channels.

2 layers/side with overlap

Average efficiency ~93% in all cases

ITk only average efficiency ~83%

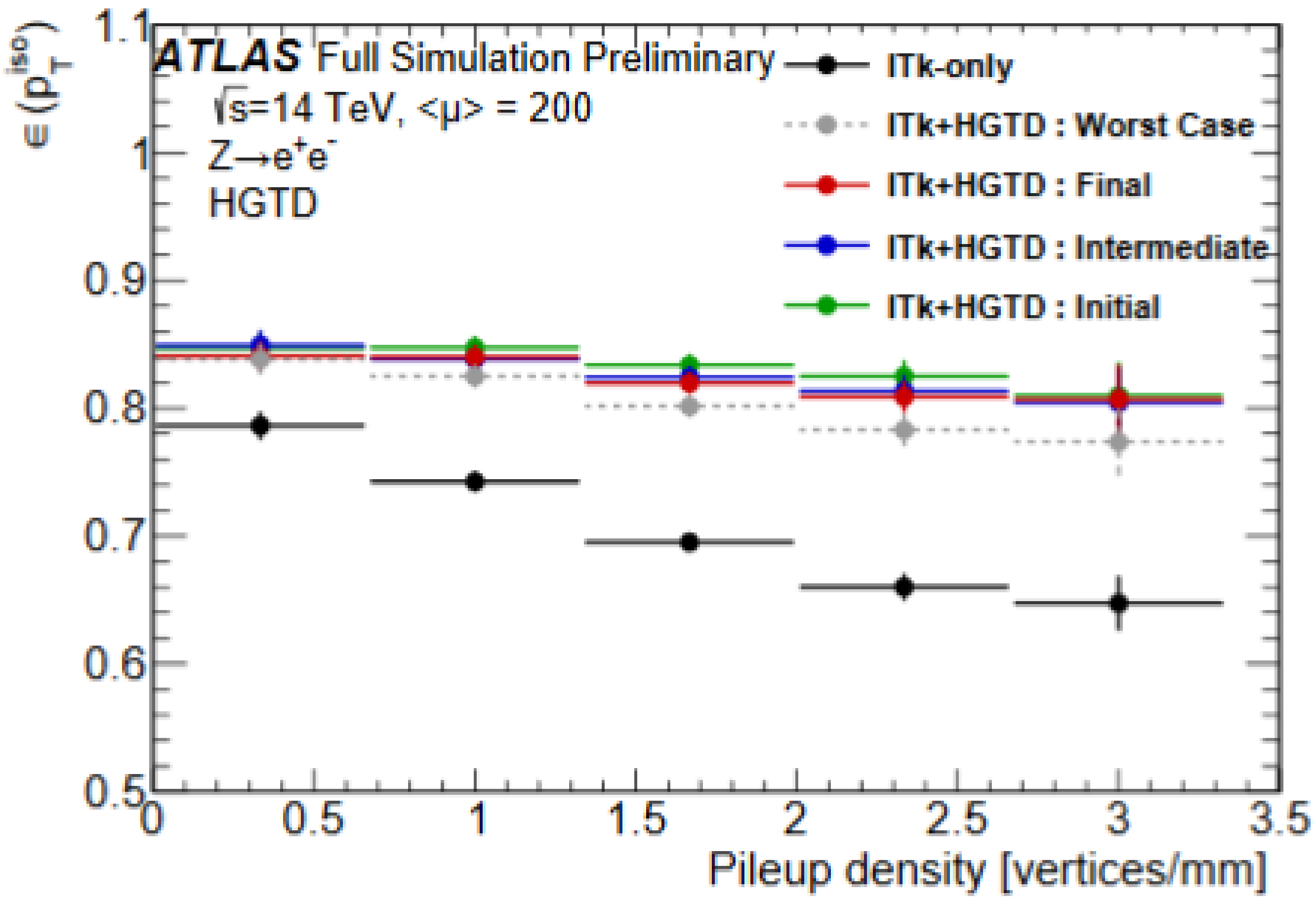

Electron ID much more uniform in rapidity with HGTD.

Some EW Physics Studies

Serious studies starting

$qqH \rightarrow qqWW^* \rightarrow qq + e\nu_e \mu\nu_\mu$

- **8% relative improvement**

  43% background rejection

  3% PU efficiency

  BDT analysis

  Top dominated background due to forward b-tagging

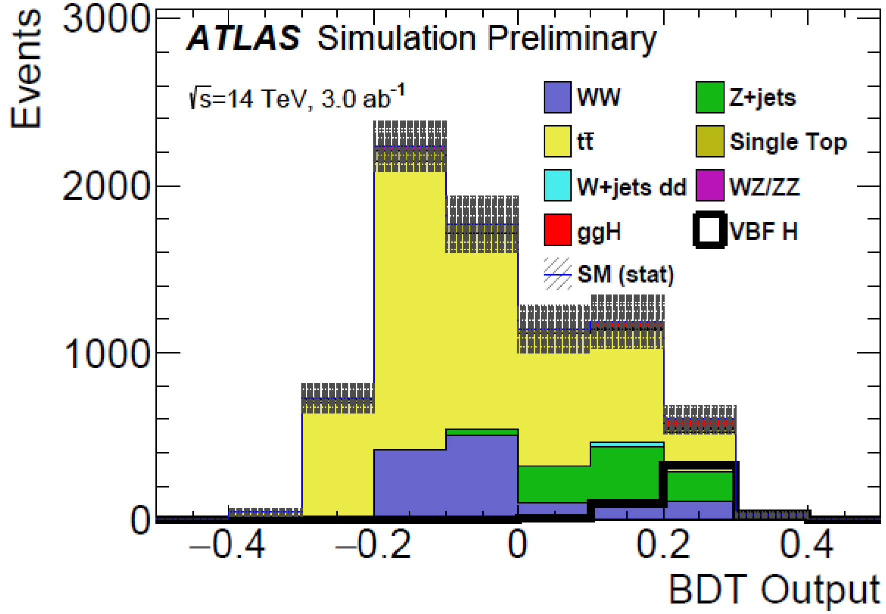

tH(→bb)

- **11% relative improvement**

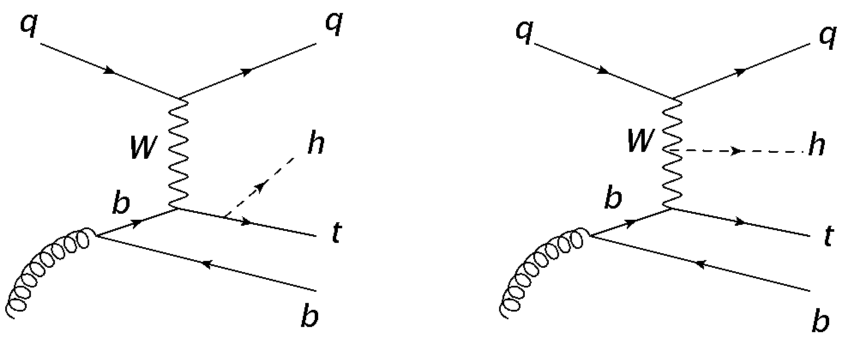

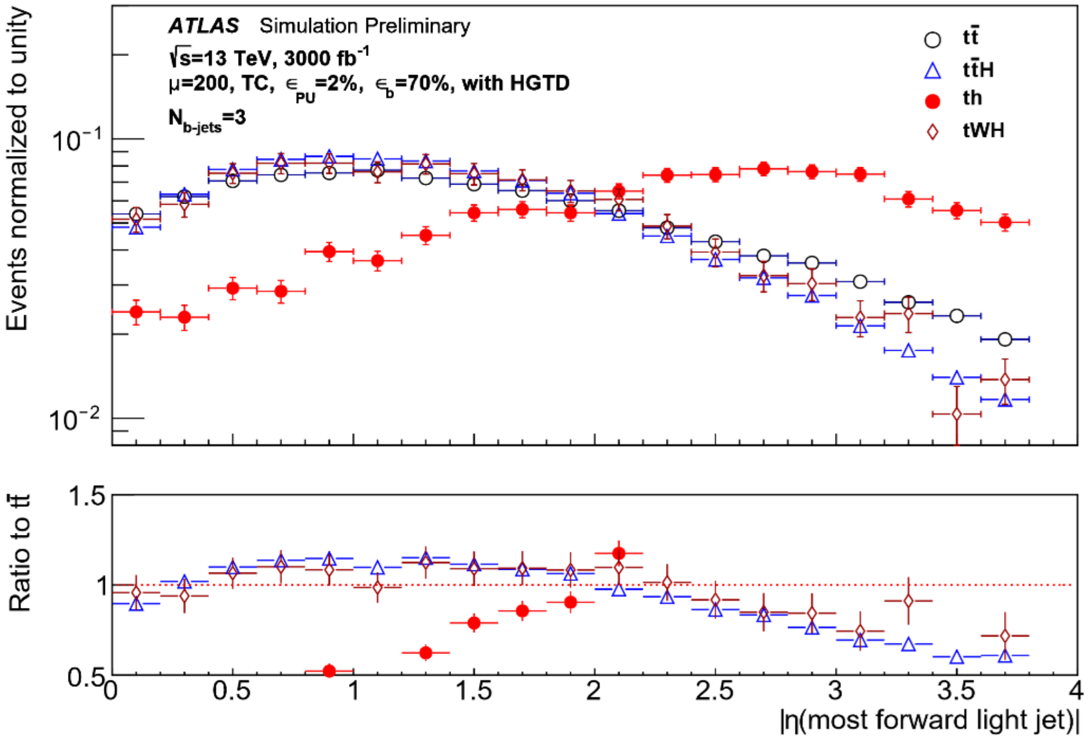

Luminosity measurement with HGTD, on- and off-line(luminometer)

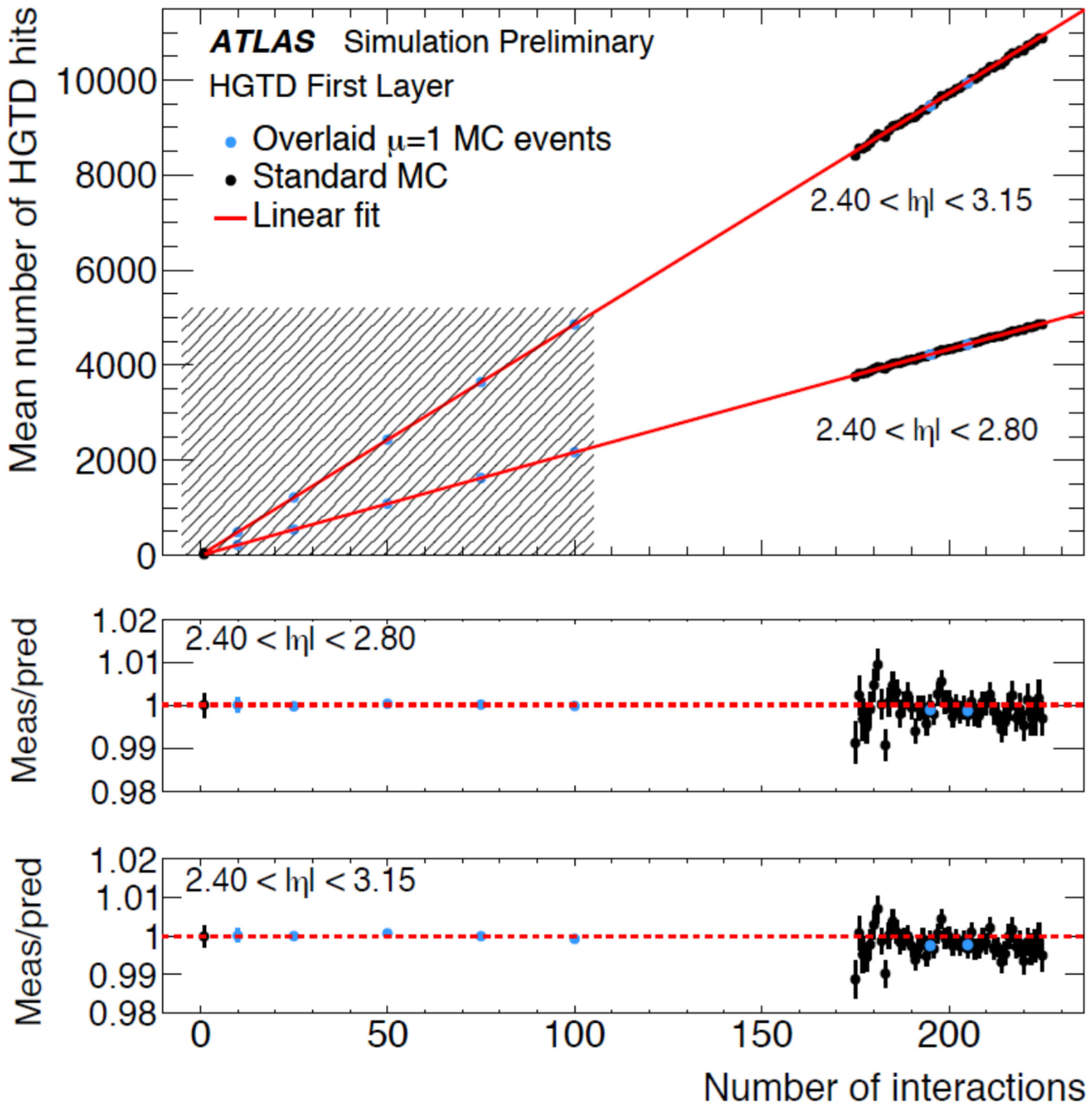

Linear dependence of number of hits on no. of interactions.

Count no. of hits for 320 mm < R < 640 mm

0.1% estimated statistical uncertainty for 1 sec integration time

Low systematics : Out of time subtraction of sideband

Hit count per ASIC and per BCID

Online:
40 MHz readout for real time estimate
Provide per BCID estimate
Total latency 440 ns (fiber 340 ns, ASIC 100 ns)

Summary

Sensors, ASIC, Integration and Radiation Hardness

Physics *Real physics studies only just started*

Promising results for pileup rejection in the high η region for object reconstruction performance
VBF and exotics will benefit, high purity for invisible searches

Sensors:

26 ps time resolution for single un-irradiated 1.3mm^2 diodes achieved
99% uniformity with low inefficiencies in the inter-pad regions
Operations up to 6e15 n_{eq}/cm^2, meeting the radiation hardness requirements
Any timing degradation due to early breakdown

Integration:

First ASIC prototypes successfully assembled at IFAE and tested in HGTD September CERN testbeam
Validate full ASIC design and expect first prototype at the last quarter of 2018

Outlook

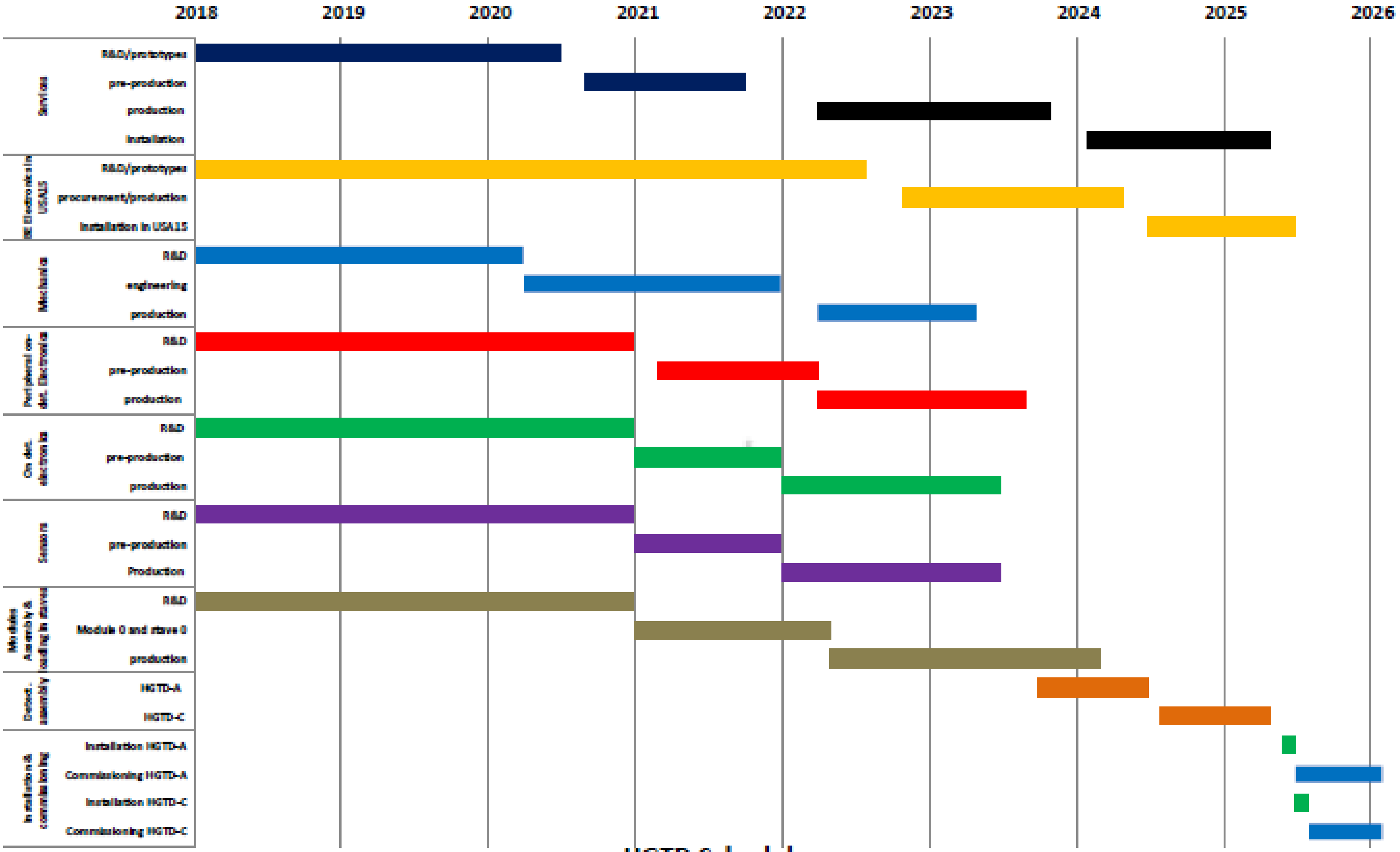

HGTD Schedule

Extra Slides

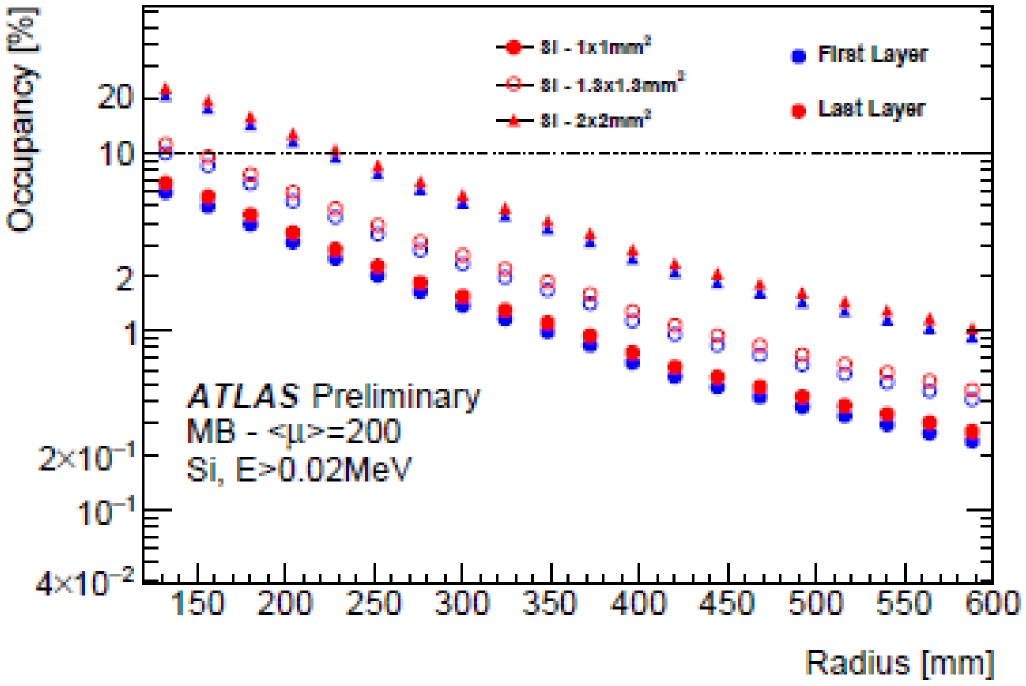

The occupancy as a function of the radius for different pixel sizes at a pileup of <μ> = 200. The occupancy for pixels of 1:3 1:3 mm^2 is the result of an interpolation.

The orientation of the readout rows for the first and second cooling plates separately, and the overlay of both.

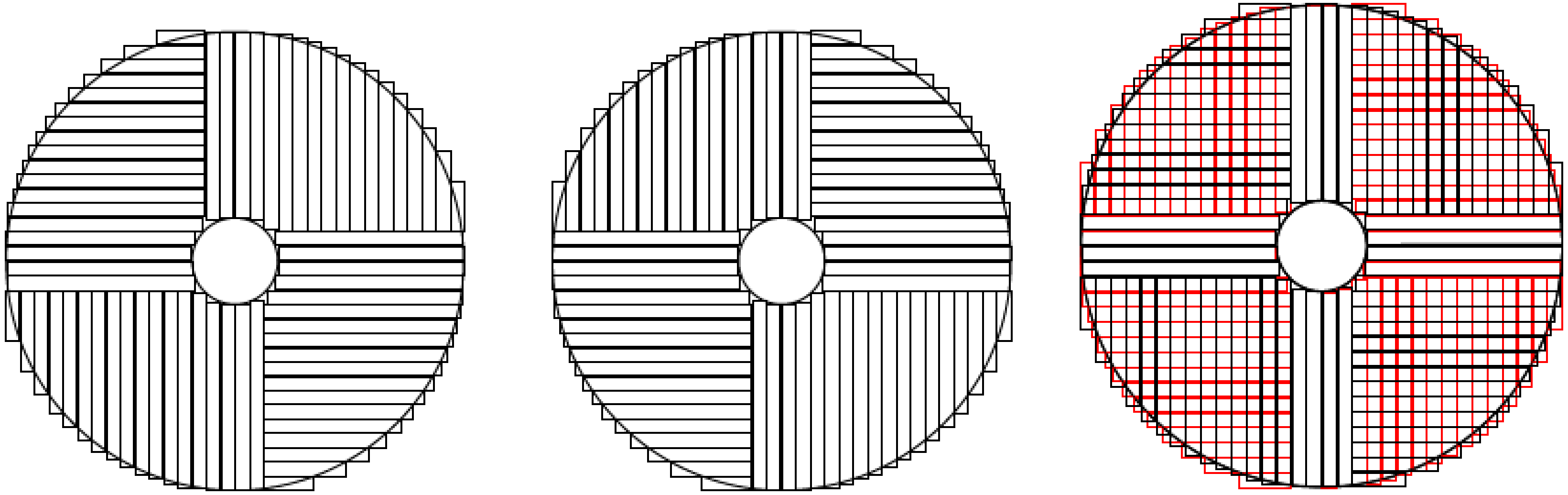

(a) First cooling disk (b) Second cooling disk (c) Overlay

Radiation Hardness :

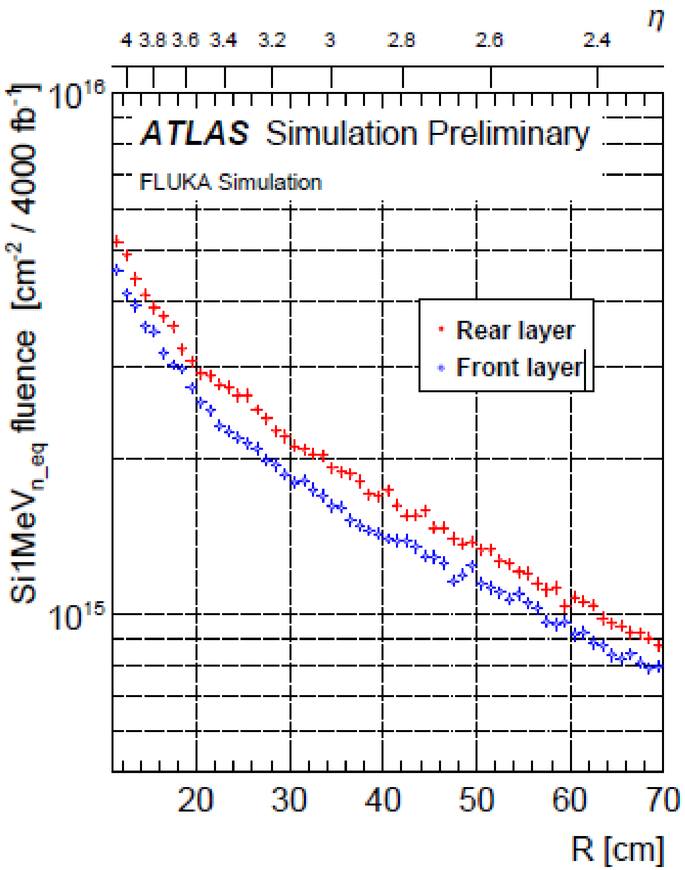

Simulation

- Similar results Fluka - GCALOR
- Max. (η = 4.0) after 4000 fb^{-1} ~ 4.9 x 10^{15} n_{eq}/cm^2 (mid cycle replacement at 2 x 10^{15})

  (Safety factor not included)

J. Lange, et al., JINST 12 (2017) P05003

σ_t vs bias voltage

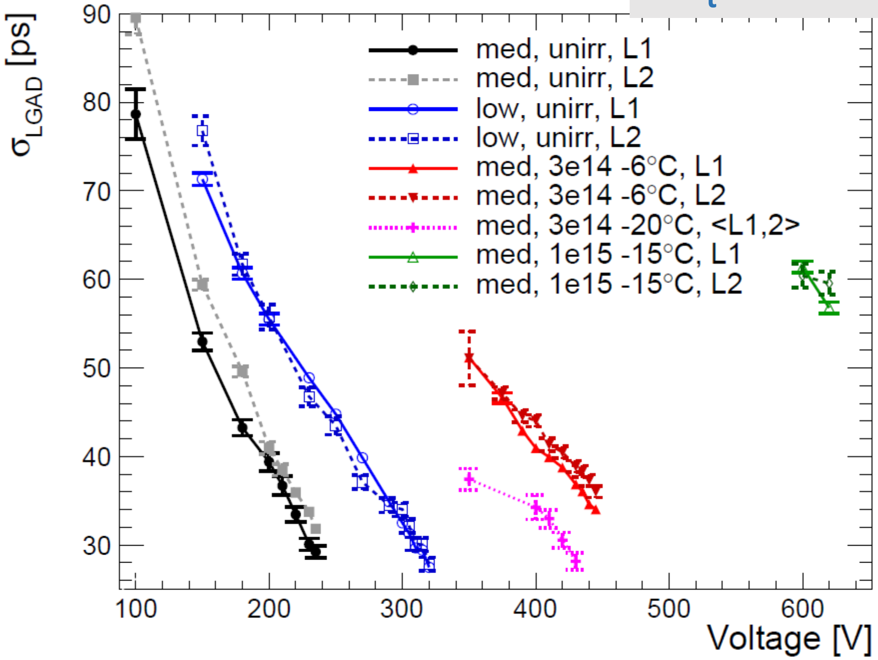

σ_t vs gain

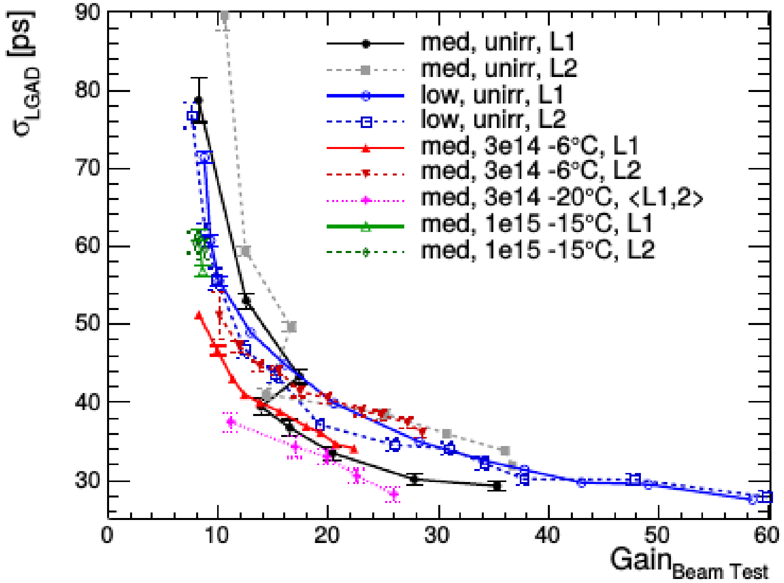

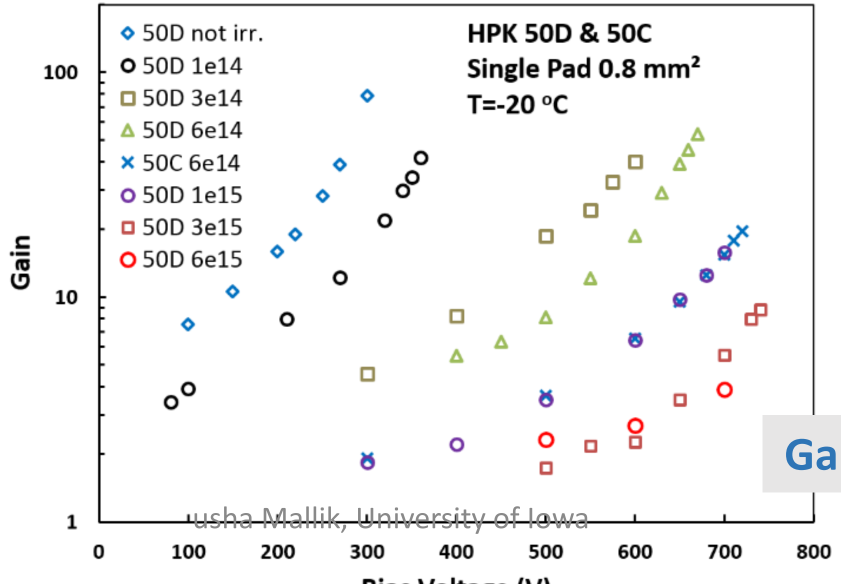

Gain vs bias voltage

Organization of the HGTD as well as location of peripheral electronics.

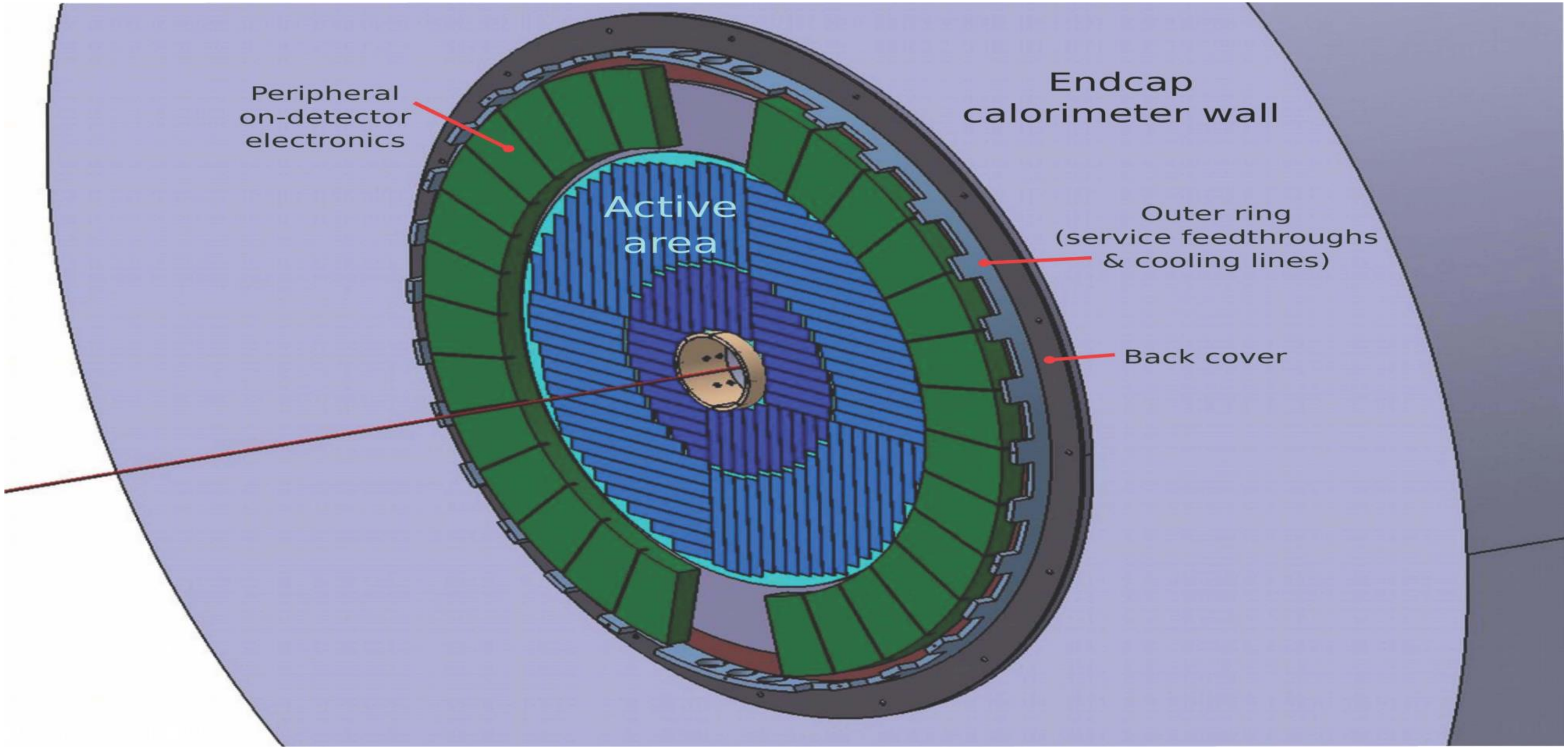

Note: Detector has two layers in order to provide the desired 30 psec resolution per track as well as redundancy. Individual sensors organized into staves and attached to cooling structures. Uses both sides of cooling structure for overlap. Outer region (light blue) to be used for luminosity monitor. Inner region (dark blue) planned to be replaced once.

Radiation Hardening of the LGAD

Radiation defects tend to remove effect of boron (acceptor removal) in the gain layer. Mainly a problem for fluences beyond 10^{15} neq/cm^2 (5×10^{15} corresponds to about 10 years of HL-LHC running at 12 cm radius). Approaches to mitigating this being investigated: Radiation tolerance and performance being tested both by MC (Fluka) and by irradiation.

- Raise voltage; replacement of detector from about 12 cm to 32 cm radius once during lifetime
- Replace boron with gallium: has been shown in space applications of solar cells to be more radiation hard
- Add carbon, which tends to tie up defects more readily than boron, so gain layer is less affected
- Optimize gain layer – thickness versus doping density

Initial Measurements have started; expect to complete all tests during this year. Also expect to receive full sized sensors this summer.

A lot of recent data for 35 μm thick sensor from Hamamatsu

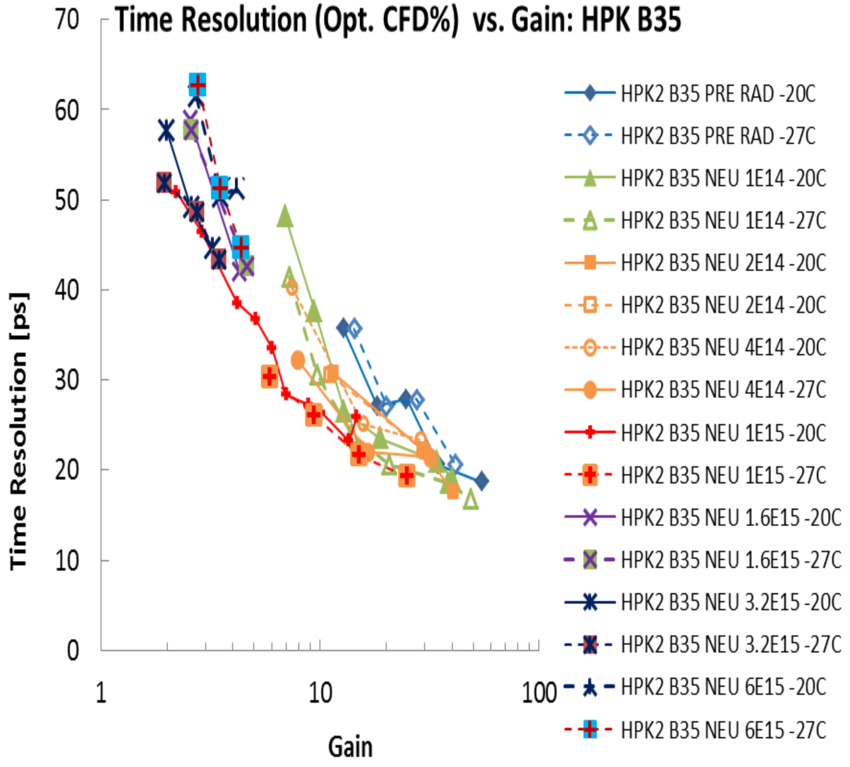

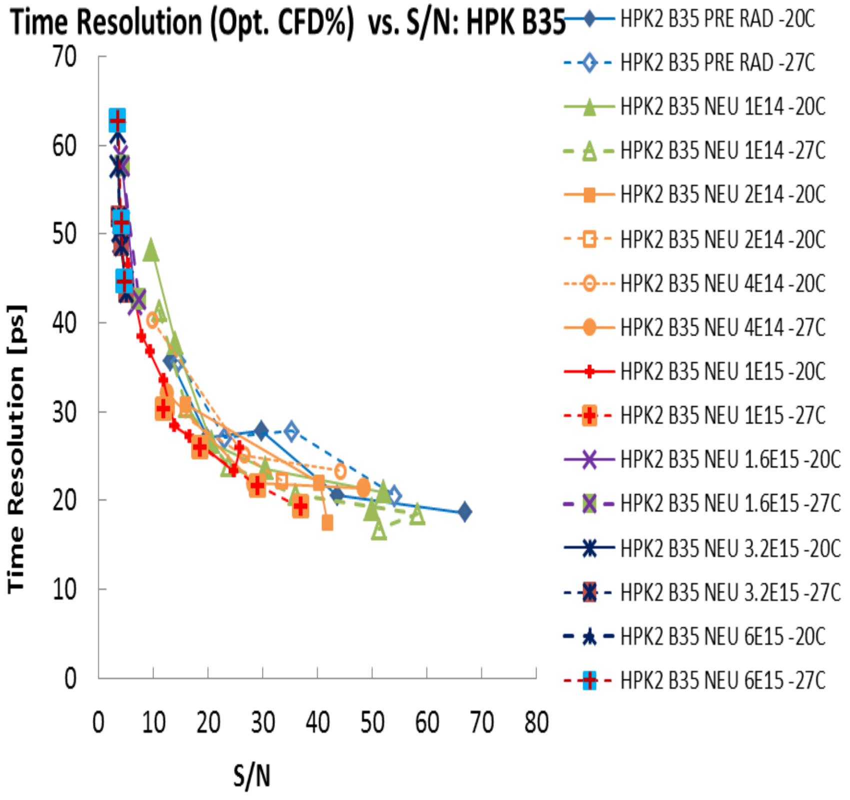

Shows time resolution achieved for a 35 micron thick sensor in a beta beam for different temperatures and fluences as a function of gain and signal (defined as peak height not total charge) to noise. Resolution levels off at about 20 psec around a gain of 20 or signal-to-noise ratio of 20. Gain is adjusted for given conditions by varying the sensor voltage. Very large gain can't be reached for very heavily irradiated sensors leading to worse resolution.

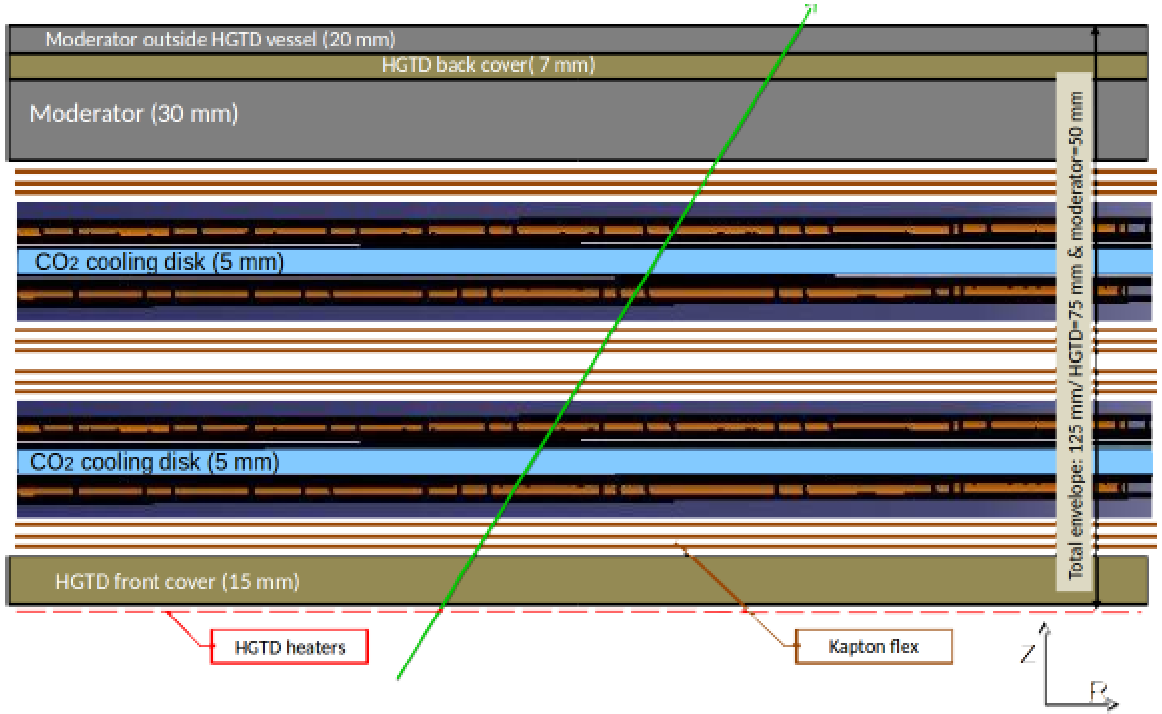

Cross section of the entire HGTD vessel including two active layers installed on the cooling plates, the front and back covers, and the moderator. An extra 20 mm moderator is located outside the vessel in close contact with the endcap cryostat.

Component	**Layer side [mm]**		**Double-sided layer [mm]**		**Total HGTD [mm]**	
	Nominal thickness	Envelope	Nominal thickness	Envelope	Nominal thickness	envelope
ASIC+sensor	1.0	1.0	2.0	2.0	4.0	4.0
Support plates	1.0	1.0	2.0	2.0	4.0	4.0
Flex circuit	2.8 - 5.5	8.0	5.6-11.0	16.0	11.2-22.0	32.0
Cooling panel	-	-	5.0	6.0	10.0	12.0
Total	7.5	10.00	20.0	26.0	40.0	52.0
Front cover	-	-	-	-	15.0	16.0
Back cover	-	-	-	-	6.0	7.0
Total HGTD					**61.0**	**75.0**
Inner moderator					30.0	30.0
Outer moderator					20.0	20.0
Total Moderator					**50.0**	**50.0**
HGTD+moderator					**111.0**	**125.0**

Estimated values of thickness per component. The nominal thickness is the manufacturing dimension of the component. The envelope is the space needed to be allocated for the component. Some components are not considered in the envelope thickness because they are included within another value. Information is given for one side of a layer (when applicable), for a double-sided layer, and the total for one HGTD side.

$$\sigma_{\mathrm{TimeWalk}} = \left[\frac{V_{th}}{\frac{S}{t_{rise}}}\right]_{\mathrm{RMS}} \propto \left[\frac{N}{\frac{dV}{dt}}\right]_{\mathrm{RMS}}, \qquad \sigma_{\mathrm{Jitter}} = \frac{N}{(dV/dt)} \simeq \frac{t_{rise}}{(S/N)},$$

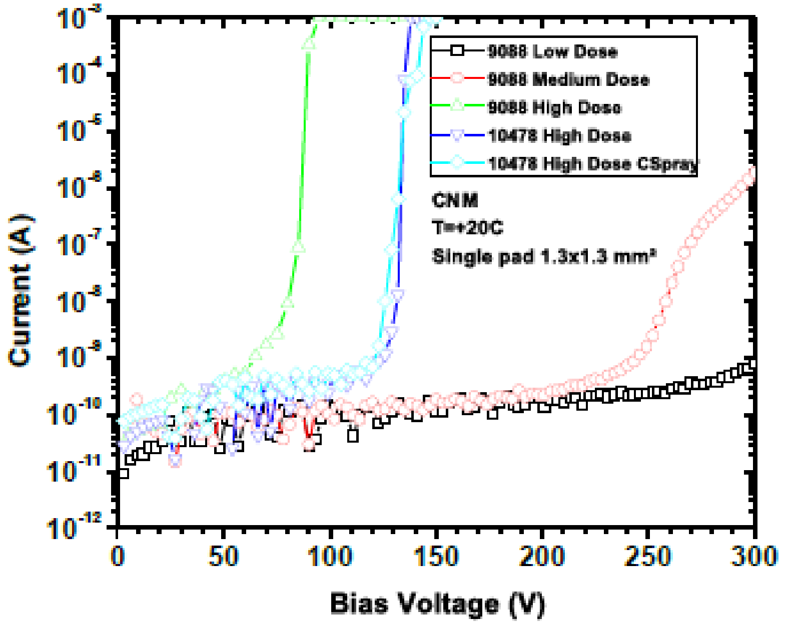

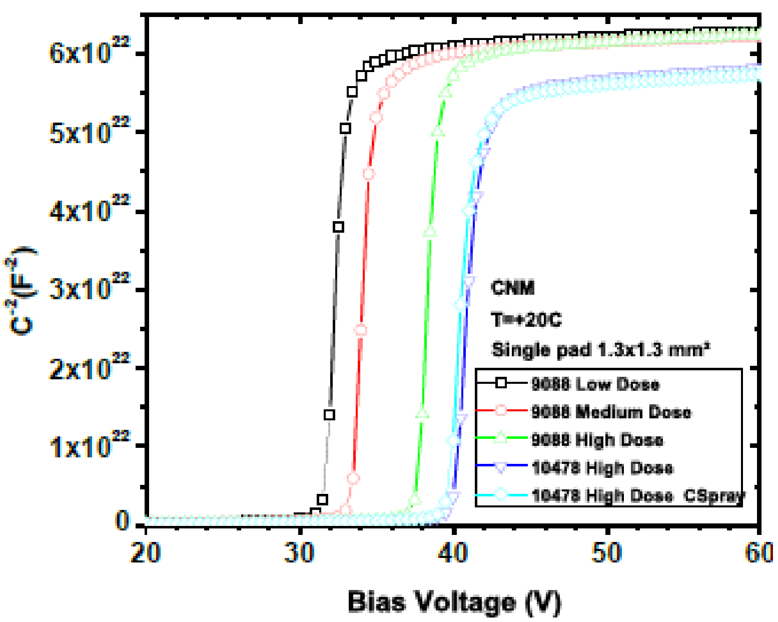

Measurements of (a) current-voltage and (b) capacitance-voltage of CNM LGA single pads from different multiplication layer doses, measured at room temperature

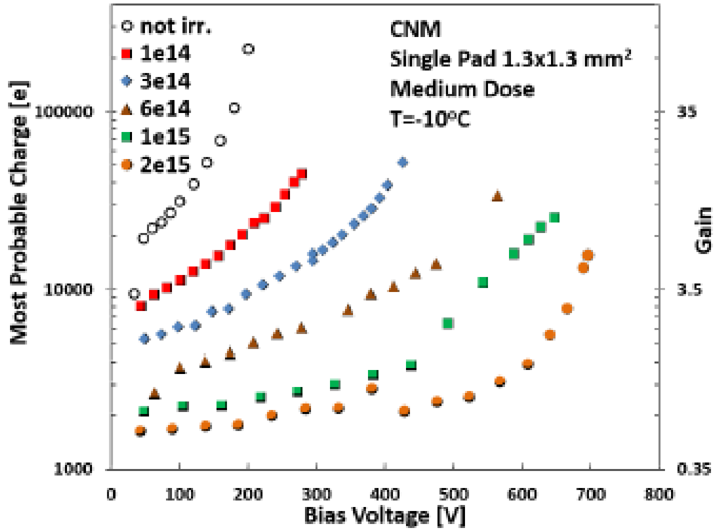

(a) CNM

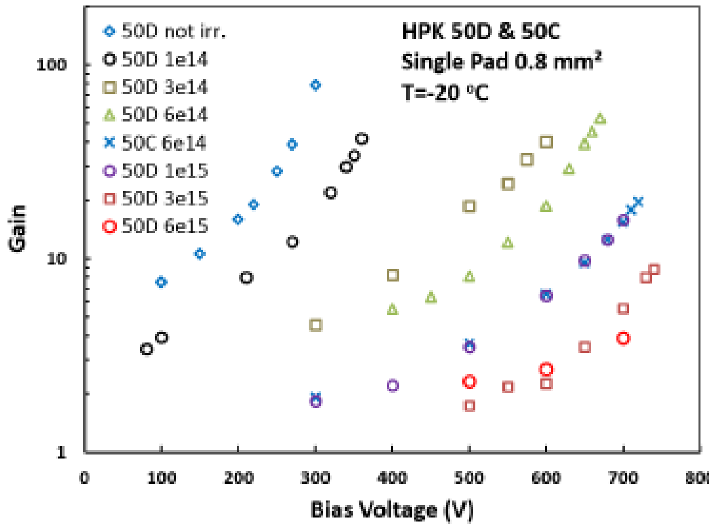

(b) HPK

Most probable charge or gain dependence on bias voltage for different fluences (in n_{eq}/cm_2) measured for (a) CNM single pads from run 9088 with medium dose and (b) HPK 50D/50C single pads

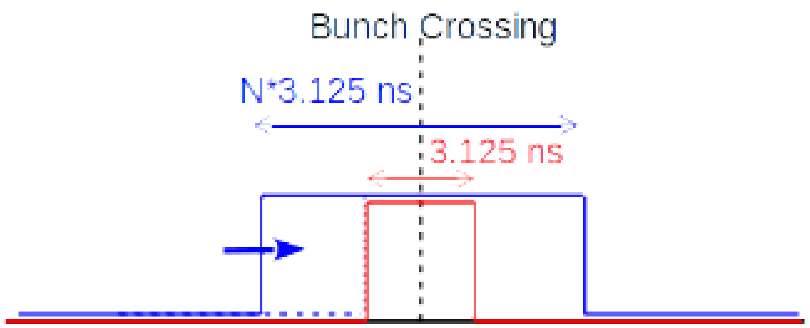

Illustration of the time windows used for counting hits for the luminosity data. The smaller window (in red) is 3.125 ns wide and is centered at the bunch crossing time. The width and relative location of the larger window (in blue) can be set in steps of of 3.125 ns through the control parameters.

Front-end ASIC requirements. The radiation levels include the safety factors defined previously and assume that the sensors and ASICs in the inner region (R ≤ 320 mm) are replaced after half of the HL-LHC program.

Pad size	1.3×1.3 mm^2
Detector capacitance	3.4 pF
TID and neutron fluence	Inner region: 4.1 MGy3.7×10^{15} n_{eq}/cm^2 Outer region: 1.6 MGy, 3.0×10^{15} n_{eq}/cm^2
Number of channels/ASIC	225
Collected charge (1 MIP) at gain=20	9.2 fC
Dynamic range	1-20 MIPs
(preamplifier+discr.) jitter at gain = 20	< 20 ps
Time walk contribution	< 10 ps
TDC binning	20 ps (TOA, TZ TOT), 40 ps (VA TOT)
TDC range	2.5 ns (TOA), 5 ns (TZ TOT), 10 ns (VA TOT)
Number of bits / hit	7 for TOA and 9 for TOT
Luminosity counters per ASIC	7 bits (sum) + 5 bits (outside window)
Total power per area (ASIC)	<300 mW/cm^2 (<1.2 W)
e-link driver bandwidth	320 Mb/s, 640 Mb/s or 1.28 Gb/s
Latency for L0/L1 triggering	10/35 μs

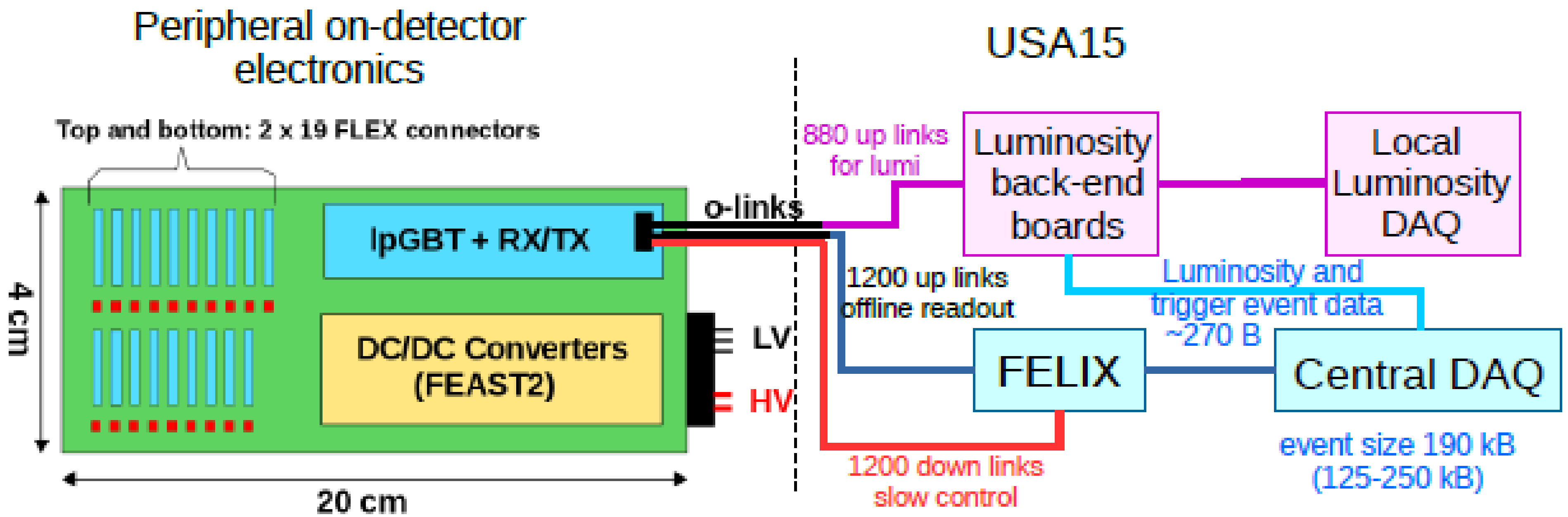

Possible implementation of the peripheral on-detector electronics for the longest readout row, and the readout chain. The flex connectors are located on the left; on the top right, the data transmitters and optical modules (lpGBT + VL + OM). The DC-DC converters are on the bottom right, where the low and high voltage connectors are. Three sets of optical links are connected to the lpGBT. The down links for slow control (in red) are connected to the FELIX boards in USA15, as well as the up links for the offline data readout. The up links with the luminosity information go to dedicated back-end boards.

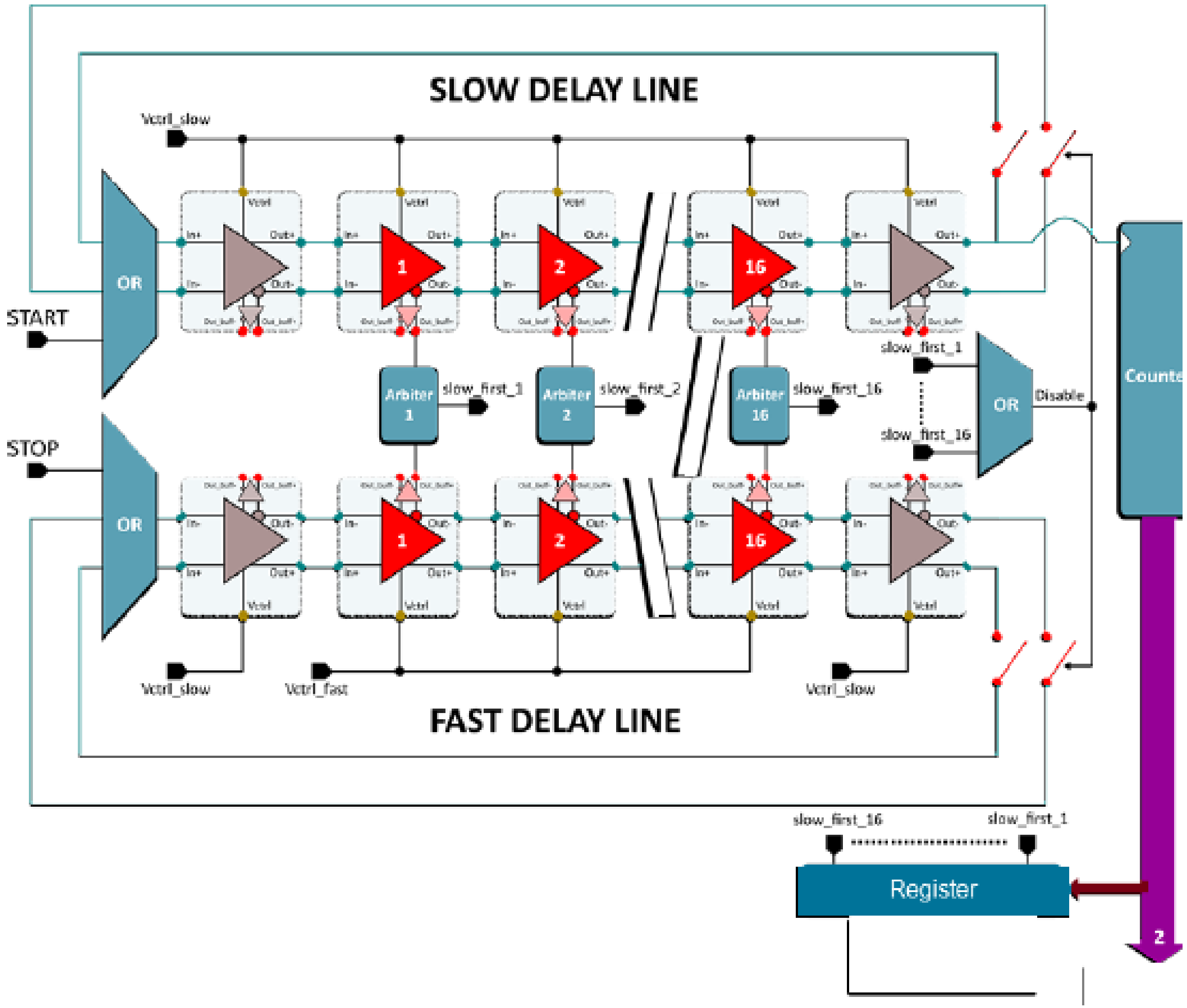

Schematics for the TDC showing the 'slow' delay line and the 'fast' delay line. The 20 ps speed difference between the two is used to provide the 20 ps time measuring bins

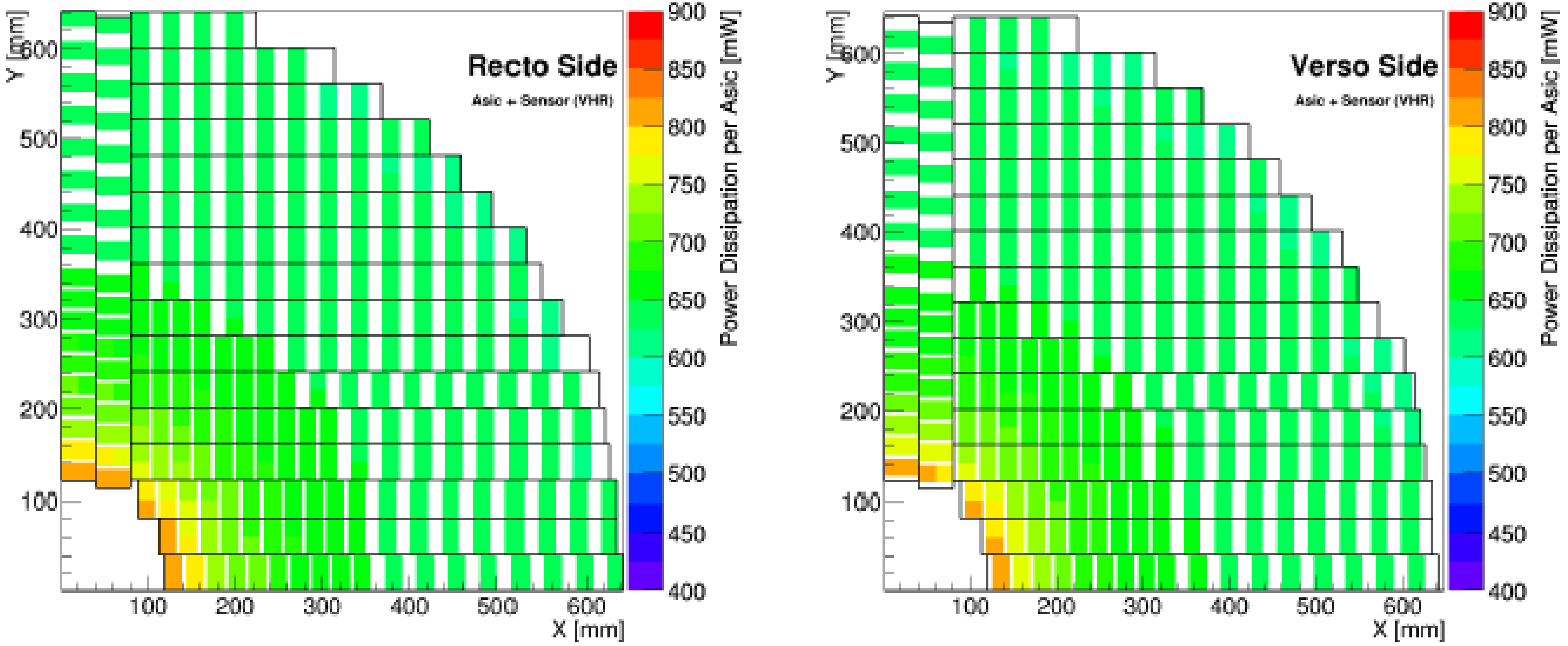

(a) Front view

(b) Back view

Power dissipation of the AS
and sensor combined, show
per ASIC, for each side of a
cooling disk.

Component	Power consumption	Total [kW]	Maximal [kW]
Sensor	< 30 mW/cm^2	1.9	1.9
ASIC	<175 mW/cm^2	8.5	12.8
Flex cable	< 100 mW/flex	0.5	1.1
HGTD cold vessel heaters	75 W/m^2-175 W/m^2	0.33	0.33
EC calorimeter cryostat heaters	120 W/m^2, 50% up to R = 1600 mm	< 0.6	0.6
Peripheral on-detector electronics	dominated by DC/DC converter	3.25	4.9
Total for CO_2 cooling		15.1	21.6

Power consumption estimations of the various HGTD components and the total for the HGTD (for a total number of 7888 flex cables, 7888 sensors of 20 × 40 mm^2 each; 6.3^2 in total and 15776 ASICS). The last column includes a safety factor of 1.5 for the electronics.

HGTD: – twentyone Institutes

- **CERN**
- **France (3):**
  - LAL/Orsay
  - LPNHE/Paris
  - Omega/Paris
- **Germany (2):**
  - Justus-Liebig-Univ., Giessen
  - Johannes-Gutenberg-Univ. of Mainz
- **Russia (1) :**
  - JINR/Dubna
- **Morocco (1):**
  - Univ. Hassan II-Casa Blanca/Morroco
- **Slovenia (1):**
  - IJS/Ljubljana

Spain (2):
- CNM-IMB-CSIC/Barcelona
- IFAE/Barcelona

Sweden (1):
- KTH /Stockholm

Taiwan (2):
- Academia Sinica/Taipei
- National Tsing-Hua University

United States DOE +NSF (7)
- BNL/Upton
- SLAC/Stanford
- Ohio State Univ. /Ohio
- SMU/Dallas
- Univ. of California Santa Cruz/Santa Cruz
- Univ. of Iowa/Iowa City
- State Univ. of NY at Stony Brook/NY